Chapter 6

Michael Kaschke, Karl-Heinz Donnerhacke
and Michael Stefan Rill

Layout by Kerstin Willnauer

Optical Visualization, Imaging, and Structural Analysis

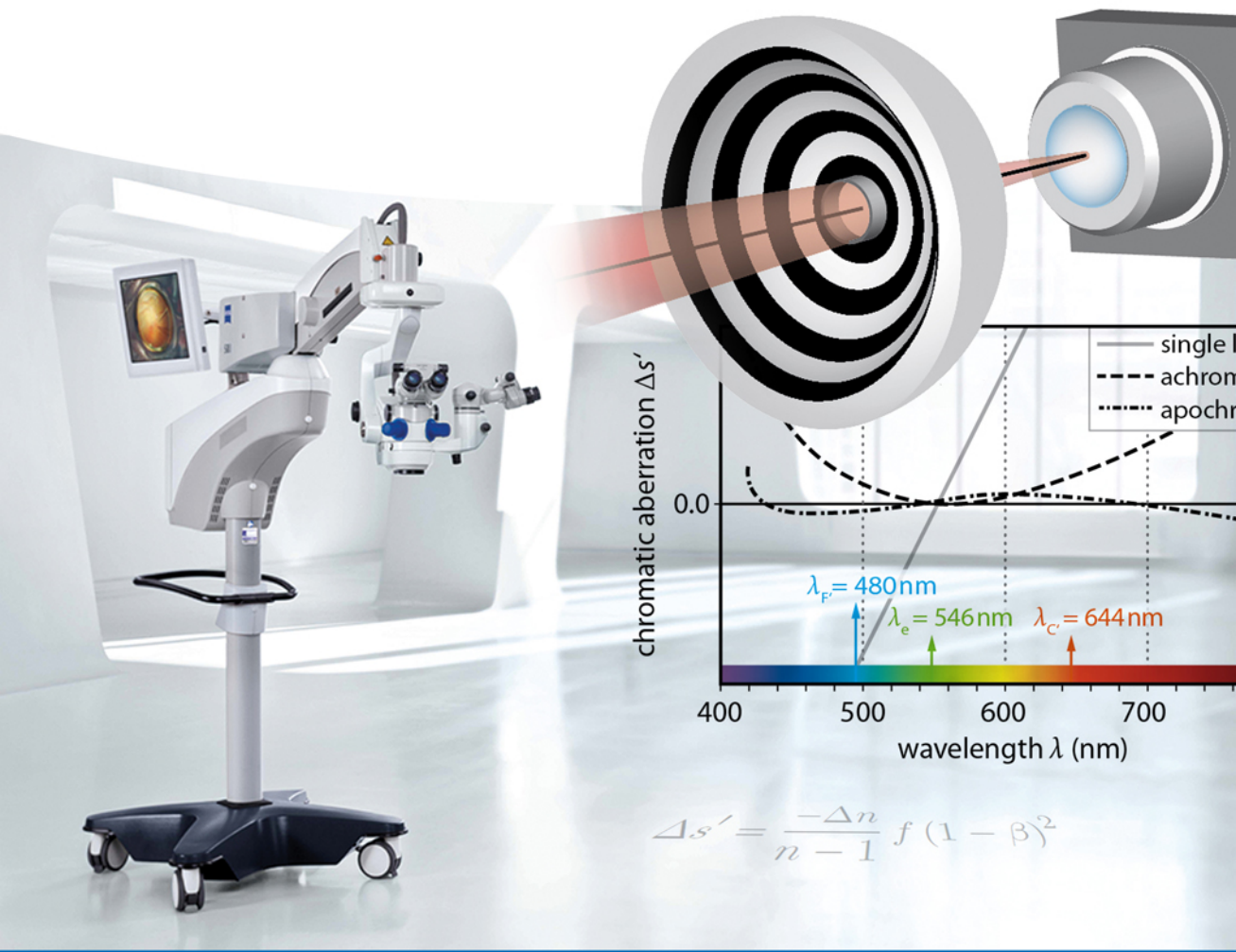

$$\Delta s' = \frac{-\Delta n}{n-1} f\,(1-\beta)^2$$

Contents

P6.1
Loupes

1. Derive Eq. (6.1) using the geometry shown in Figure 6.1.
2. Calculate the magnification of a loupe which consists of a thin lens with a focal length of $f = 25\,\text{mm}$. Please consider the following cases
   - Alter the distance L_{LP} between the observer's eye and the loupe from $L_{\text{LP}} = 0\,\text{mm}$ to $100\,\text{mm}$.
   - Place an object in the focus of the lens. How does the resolution of the eye change? At first, determine the magnification and resolution of an eye without visual aids for the near point at the typical near viewing distance $s_{\text{nv}} = 250\,\text{mm}$. At this distance from the loupe, the eye has a focal length of $17\,\text{mm}$. The density of rods in the fovea is approximately $100/\text{mm}$.
   - Why are loupes with a magnification of $100\times$ not available? Where is the limit?
3. The field of view d_{fov} of a simple magnifier lens can be calculated via

$$d_{\text{fov}} = \frac{d_{\text{L}}}{L_{\text{LP}}\,\mathcal{D}_{\text{L}}^{*}} \ , \tag{6.79}$$

   in which $\mathcal{D}_{\text{L}}^{*}$ is the effective optical power of a magnifier lens given by

$$\mathcal{D}_{\text{L}}^{*} = \frac{\mathcal{D}_{\text{L}} - 1/s'}{1 - L_{\text{LP}}/s'} \ . \tag{6.80}$$

   Derive Eq. (6.79) and determine an approximation for d_{fov} as a function of only the power of the lens.
4. Calculate the parameters of Table 6.1 for a bi-convex spherical lens with a refractive index of $n = 1.7$. Is the assumption of a thin lens justified? What differences can you observe?
5. How can β_{L} and d_{fov} be derived for each magnifier lens with $\mathcal{D}_{\text{L}}$ and d_{L} given an optimum working condition?

Solution:

1. We want to derive Eq. (6.1) for the angular magnification of a loupe in front an eye which is given by

$$\beta_{\text{L}} = \frac{\tan\gamma'}{\tan\gamma} = -\mathcal{D}_{\text{L}} s_{\text{ref}} + A_{\text{set}}\, s_{\text{ref}}\,(1 - \mathcal{D}_{\text{L}} L_{\text{LP}}) \ . \tag{6.1}$$

   Using Figure S6.1, we can write

$$\beta_{\text{L}} = \frac{\tan\gamma'}{\tan\gamma} = \frac{h'_{\text{I,L}}/L_{\text{IP}}}{-h_0/s_{\text{ref}}} = \frac{h'_{\text{I,L}}}{h_0} \cdot \frac{s_{\text{ref}}}{L_{\text{IP}}} \ . \tag{S6.1}$$

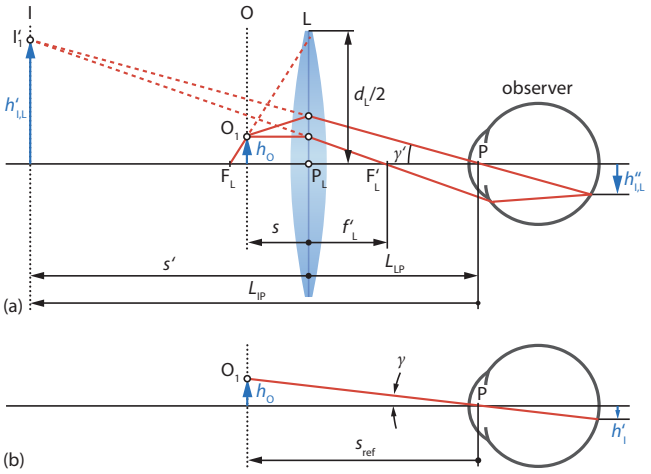

Figure S6.1 (a) Ray diagram illustrating the magnification of a magnifier loupe. (b) Object observed without a lens.

Here, we note that $s_{\mathrm{ref}} < 0$ (by definition) and $L_{\mathrm{IP}} < 0$, whereas $L_{\mathrm{LP}} > 0$. The magnification of a lens is given by Eq. (A15) and can be expressed by means of the imaging equation of a lens (A14) by making use of $\mathcal{D}_{\mathrm{L}} = 1/f'$ (note that $s' = L_{\mathrm{LP}} + L_{\mathrm{IP}} < 0$). Thus, we have

$$\beta_{\mathrm{lens}} = \frac{h'_{\mathrm{I,L}}}{h_0} = \frac{s'}{s} = 1 - \mathcal{D}_{\mathrm{L}} s' \quad . \tag{S6.2}$$

Assuming that the accommodation of the eye (Chapter 2, Eq. (2.9)) is equal to the apparent distance of the image, we can write

$$A_{\mathrm{set}} = \frac{1}{L_{\mathrm{IP}}} \quad .$$

Thus, we obtain with Eqs. (S6.1) and (S6.2)

$$\begin{aligned}
\beta_{\mathrm{L}} &= \frac{\tan\gamma'}{\tan\gamma} \\
&= \frac{h'_{\mathrm{I,L}}}{h_0} \cdot \frac{s_{\mathrm{ref}}}{L_{\mathrm{IP}}} \\
&= \beta_{\mathrm{lens}} \cdot \frac{s_{\mathrm{ref}}}{L_{\mathrm{IP}}} \\
&= (1 - \mathcal{D}_{\mathrm{L}} s') \frac{s_{\mathrm{ref}}}{L_{\mathrm{IP}}} \\
&= (1 - \mathcal{D}_{\mathrm{L}} s') A_{\mathrm{set}} s_{\mathrm{ref}} \\
&= A_{\mathrm{set}} s_{\mathrm{ref}} - A_{\mathrm{set}} \mathcal{D}_{\mathrm{L}} (L_{\mathrm{LP}} + L_{\mathrm{IP}}) s_{\mathrm{ref}} \\
&= A_{\mathrm{set}} s_{\mathrm{ref}} - A_{\mathrm{set}} \mathcal{D}_{\mathrm{L}} L_{\mathrm{LP}} s_{\mathrm{ref}} - A_{\mathrm{set}} \mathcal{D}_{\mathrm{L}} L_{\mathrm{IP}} s_{\mathrm{ref}} \\
&= -A_{\mathrm{set}} \mathcal{D}_{\mathrm{L}} L_{\mathrm{IP}} s_{\mathrm{ref}} + A_{\mathrm{set}} s_{\mathrm{ref}} - A_{\mathrm{set}} \mathcal{D}_{\mathrm{L}} L_{\mathrm{LP}} s_{\mathrm{ref}}
\end{aligned}$$

and finally

$$\beta_{\mathrm{L}} = -\mathcal{D}_{\mathrm{L}} s_{\mathrm{ref}} + A_{\mathrm{set}} s_{\mathrm{ref}} (1 - \mathcal{D}_{\mathrm{L}} L_{\mathrm{LP}}) \ .$$

In the special case that we have $s_{\mathrm{ref}} = s_{\mathrm{nv}} = -250\,\mathrm{mm}$ and $L_{\mathrm{LP}} = f' = 1/\mathcal{D}_{\mathrm{L}}$, we obtain for the nominal magnification of a loupe

$$\begin{aligned} \beta_{\mathrm{L,nominal}} &= -\mathcal{D}_{\mathrm{L}}(-250\ \mathrm{mm}) + A_{\mathrm{set}} s_{\mathrm{ref}} \left(1 - \mathcal{D}_{\mathrm{L}} \frac{1}{\mathcal{D}_{\mathrm{L}}}\right) \\ &= \mathcal{D}_{\mathrm{L}} \cdot 0.25\ \mathrm{m} = \frac{\mathcal{D}_{\mathrm{L}}}{4\mathrm{D}} \ . \end{aligned} \tag{6.2}$$

2. The (angular) magnification is defined by the ratio of the tangent of the viewing angles with and without the magnifier

$$\beta = \frac{\tan \gamma'}{\tan \gamma} \ ,$$

in which γ is the visual angle without the loupe and the object at the reference viewing distance. We set $s_{\mathrm{ref}} = -s_{\mathrm{nv}} = -250\,\mathrm{mm}$ and obtain

$$\tan \gamma = \frac{h_0}{s_{\mathrm{ref}}} \ .$$

With the lens equation (A14) for the magnifier lens

$$\frac{1}{s'} - \frac{1}{s} = \frac{1}{f'} \ ,$$

we can write the tangent of the angle γ with magnifying lens, image distance s' (note: $s' < 0$, since the image is virtual), and loupe distance from the eye L_{LP} as

$$\tan \gamma = \frac{h'_{\mathrm{I,L}}}{L_{\mathrm{IP}}} = \frac{h'_{\mathrm{I,L}}}{s' - L_{\mathrm{LP}}} \ .$$

Next, we use for the magnification of the lens Eq. (6.2) and find

$$\begin{aligned} \beta &= \frac{\tan \gamma'}{\tan \gamma} \\ &= \left(\frac{h'_{\mathrm{I,L}}}{s' - L_{\mathrm{LP}}}\right) \frac{s_{\mathrm{ref}}}{h_0} \\ &= \left(\frac{f' - s'}{s' - L_{\mathrm{LP}}}\right) \frac{s_{\mathrm{ref}}}{f'} \ . \end{aligned}$$

If the object is located in the focal plane, $s = f' = 25\,\mathrm{mm}$ and thus $s' \to -\infty$. With an accommodation for the unaided eye at near viewing distance $s_{\mathrm{ref}} = -s_{\mathrm{nv}} = -250\,\mathrm{mm}$, we calculate

$$\begin{aligned} \beta_0 &= \lim_{s' \to -\infty} \left(\frac{f' - s'}{s' - L_{\mathrm{LP}}}\right) \cdot \frac{s_{\mathrm{ref}}}{f'} \\ &= \lim_{s' \to \infty} \left(\frac{f'/s' - 1}{1 - L_{\mathrm{LP}}/s'}\right) \cdot \frac{s_{\mathrm{ref}}}{f'} = \frac{s_{\mathrm{nv}}}{f'} = 10\times \ . \end{aligned}$$

Table S6.1 Magnification for different values of the eye-loupe distance L_{LP}.

L_{LP} (mm)	β
0	11
10	10.6
25	10 (nominal magnification)
50	9
100	7

When the distance between loupe and eye has an arbitrary value L_{LP}, but the eye still accommodates to the reference viewing distance s_{ref}, we have

$$s' = L_{\mathrm{LP}} + s_{\mathrm{ref}} \ . \tag{S6.3}$$

The magnification thus yields

$$\begin{aligned}
\beta &= \frac{\tan\gamma}{\tan\gamma_0} \\
&= \left(\frac{f' - s'}{s' - L_{\mathrm{LP}}}\right) \cdot \frac{s_{\mathrm{ref}}}{f'} \\
&= 1 - \frac{s_{\mathrm{ref}}}{f'} - \frac{L_{\mathrm{LP}}}{f'} \\
&= 1 + \beta_0 - \frac{L_{\mathrm{LP}}}{f'} \ .
\end{aligned}$$

Specific values of the magnification for different distances are given in Table S6.1.

The given density of rods of 100/mm corresponds to an average distance between rods of $\Delta x = 0.01\,\mathrm{mm}$ on the retina. At the near point of the eye with the given focal length of the eye $f_{\mathrm{eye}} = 17\,\mathrm{mm}$, we obtain the smallest resolvable angle determined by the rod density:

$$\gamma_{\mathrm{min,eye}} = \frac{\Delta x}{f_{\mathrm{eye}}} = 0.000588\ \mathrm{rad} = 2.02' \ .$$

For a loupe with magnification β, this angle is magnified by a factor of β. Thus, the minimum resolvable angle using a loupe of magnification β becomes

$$\Delta\gamma_{\mathrm{min,loupe}} = \frac{\gamma_{\mathrm{min,eye}}}{\beta} \ .$$

The pupil of the eye is about 3.6 mm behind the cornea inside the eye. Therefore, there cannot be any loupe with a focal length $f' < 3.6\,\mathrm{mm}$, as such a loupe could simply be not close enough to the eye pupil. At best, $f' = 5\,\mathrm{mm}$ is imaginable, and this corresponds to a magnification of $\beta_0 = -s_{\mathrm{ref}}/f' = 50\times$ under the assumption of an non-accommodated observing eye.

More critical however is another limitation. In order to have a sufficient field of view, the loupe should have a clear diameter of $d_{\mathrm{lens}} \approx 1\,\mathrm{cm}$. With an aperture ratio of $d_{\mathrm{lens}}/f' = 0.5$, this corresponds to a focal length of $20\,\mathrm{mm}$. In this case, we will get significant imaging errors (aberrations). For $d_{\mathrm{lens}}/f' = 1$ and $\beta_0 = 25\times$, the lens will almost have a spherical shape.

3. We start from Eq. (S6.2), that is,

$$\beta_{\mathrm{lens}} = \frac{s'}{s} = 1 - \mathcal{D}_{\mathrm{L}} s' \quad .$$

Since the maximum size of the virtual image d'_{fov} of the object is limited by the size of the lens aperture d_{lens}, we can write (note that $s' < 0$)

$$\frac{d_{\mathrm{lens}}}{d'_{\mathrm{fov}}} = \frac{L_{\mathrm{LP}}}{L_{\mathrm{LP}} - s'}$$

and further

$$d'_{\mathrm{fov}} = \frac{d_{\mathrm{lens}}(L_{\mathrm{LP}} - s')}{L_{\mathrm{LP}}} \quad .$$

The maximum size of the virtual image d'_{fov} corresponds to a maximum field of view at the object of

$$\frac{d'_{\mathrm{fov}}}{d_{\mathrm{fov}}} = \beta_{\mathrm{lens}} = 1 - \mathcal{D}_{\mathrm{L}} s' \quad .$$

As a consequence, we obtain Eq. (6.79) given by

$$d_{\mathrm{fov}} = \frac{d'_{\mathrm{fov}}}{1 - \mathcal{D}_{\mathrm{L}} s'} = \frac{d_{\mathrm{lens}}(L_{\mathrm{LP}} - s')}{L_{\mathrm{LP}}(1 - \mathcal{D}_{\mathrm{L}} s')} = \frac{d_{\mathrm{lens}}}{L_{\mathrm{LP}} \mathcal{D}^*_{\mathrm{L}}} \quad ,$$

where we used Eq. (6.80), that is,

$$\mathcal{D}^*_{\mathrm{L}} = \frac{1 - \mathcal{D}_{\mathrm{L}} s'}{L_{\mathrm{LP}} - s'} = \frac{\mathcal{D}_{\mathrm{L}} - 1/s'}{1 - L_{\mathrm{LP}}/s'} \quad .$$

We can find an approximation for the case that the object is in the focal plane of the loupe ($s = f'$ in $1/s' - 1/s = 1/f'$) so that $s' \to -\infty$. From Eq. (6.80) and the transition $\mathcal{D}^*_{\mathrm{L}} \to \mathcal{D}_{\mathrm{L}}$, we obtain

$$d_{\mathrm{fov}} = \frac{d_{\mathrm{lens}}}{L_{\mathrm{LP}} \mathcal{D}_{\mathrm{L}}} \quad .$$

Therefore, when the object is located at the focal plane, the field of view d_{fov} is an inverse function of the power of the lens, which means that the higher the power of the loupe the smaller the field of view.

4. We use Eq. (A12) for a bi-convex thin lens with $n = 1.7$ to calculate the radii $r_{1,2}$ of the lens surfaces. Moreover, we use Eq. (6.1) to calculate the real magnification in the case of the optimum working condition. From Table S6.2 follows that

Table S6.2 Optical parameters for some bi-convex lenses.

$\mathcal{D}_\mathrm{L}$	f'(mm)	$r_{1,2}$ (mm)	$\beta_{\mathrm{L,nominal}}$	β_L (see Eq. (S6.1))	β_L (experimental) (see also Table (6.1))
6	167	58	1.5	1.95	2.1
8	125	44	2.0	1.78	2.7
12	83	29	3.0	2.34	3.5
16	62	22	4.0	3.66	3.25
20	50	17	5.0	4.64	3.1

for high $\mathcal{D}_\mathrm{L}$, the lens radius approaches the focal length. As the lens becomes "thick", the thin lens approximation does not hold anymore. Hence, we also see that the experimentally obtained magnifications differ from the calculated ones. Another reason for the differences is that the loupes in Table 6.1 contain aspheric lenses.

5. Optimum working conditions are :
   1. Object is located in the focal plane of $f'_\mathrm{L} = L_\mathrm{LP}$ and the eye is relaxed during viewing.
   2. The reference viewing distance $|s_\mathrm{ref}|$ equals the typical near viewing distance $s_\mathrm{nv} = 25\,\mathrm{cm}$.

P6.2
Stereoscopic vision

An observer has an interpupillary distance of $\mathrm{PD} = 62\,\mathrm{mm}$. He uses a telescope with $8\times$ magnification whose objective lens is located at a distance of $115\,\mathrm{mm}$ from the eye. How much is the stereoscopic vision improved compared to the case of a "naked" eye without visual aids? Compare the minimum stereo angles ε_min for both cases.

Solution:

We start with calculating the stereoscopic effect by observation with the "naked" eye. For this purpose, we use the schematics in Figure S6.2.
The stereoscopic depth perception (given by the parameter ΔL_eye) is the ability of the eye to detect a difference in depth or distance between two object points O_1 and O_2. The minimum stereo angle ε_min (experimentally observed to be in the order of $10''$) is another expression of this depth perception. From Figure S6.2, we can easily

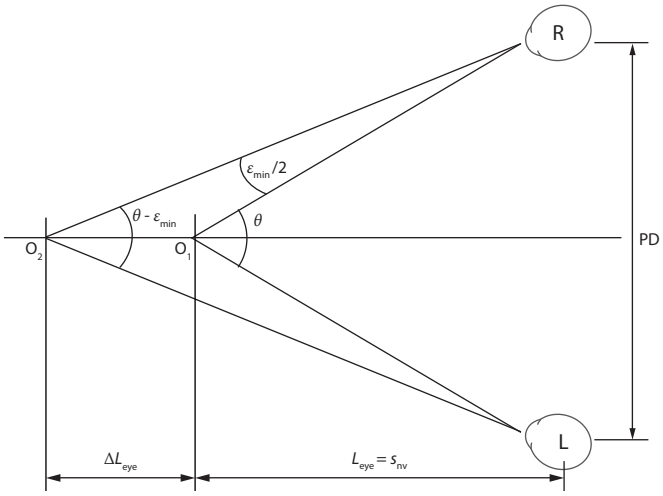

Figure S6.2 Geometry illustrating the optical concept of stereoscopic vision.

derive the following relations:

$$\theta = \frac{\mathrm{PD}}{L_{\mathrm{eye}}} \ ,$$
$$\theta - \varepsilon_{\mathrm{min}} = \frac{\mathrm{PD}}{L_{\mathrm{eye}} + \Delta L_{\mathrm{eye}}} \ . \tag{S6.4}$$

By elimination of θ (under the assumption that $\varepsilon_{\mathrm{min}} \ll \mathrm{PD}/L_{\mathrm{eye}}$), we can easily derive Eq. (2.18) or, equivalently, Eqs. (2.19) and

$$\Delta L_{\mathrm{eye}} = \frac{\varepsilon_{\mathrm{min}} \cdot L_{\mathrm{eye}}^2}{\mathrm{PD}} \ . \tag{6.14}$$

Now, we want to see how a binocular system like a binocular telescope affects the stereoscopic depth perception. This may happen either by a change of the interpupillary distance to a new stereo-base distance b (Figure S6.3) or by the magnification of the system which effectively decreases the apparent distance of the observed object. Let us calculate the combined effect. For this purpose, we take a look at Figure S6.4 in which we have depicted one imaging channel of the binocular system, which is sufficient to consider due to symmetry. Shown in the new stereo base $b/2$, we can see the object and image position O_i and O_i', respectively, and the image distances L' and $\Delta L'$. It should be noted that object O_i represents the edges of an off-axis object with size $b/2$. Such a transversally extended object is de-magnified by an afocal telescope system by a factor of $1/\beta$. This seems to be counter-intuitive, as the angular magnification of an afocal telescope is β. This can be best explained by the following reasoning: If an object at large (but finite) distance L with size h_0 is imaged through a telescope, the image will be at finite (but large) distance L/β^2. Consequently, since

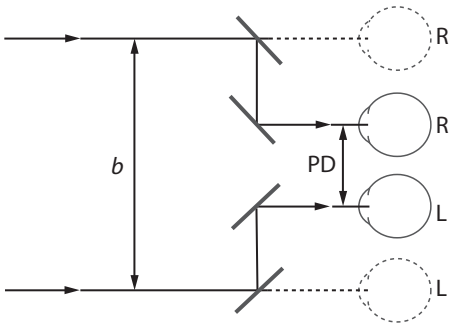

Figure S6.3 Change of the interpupillary distance to a new stereo base b.

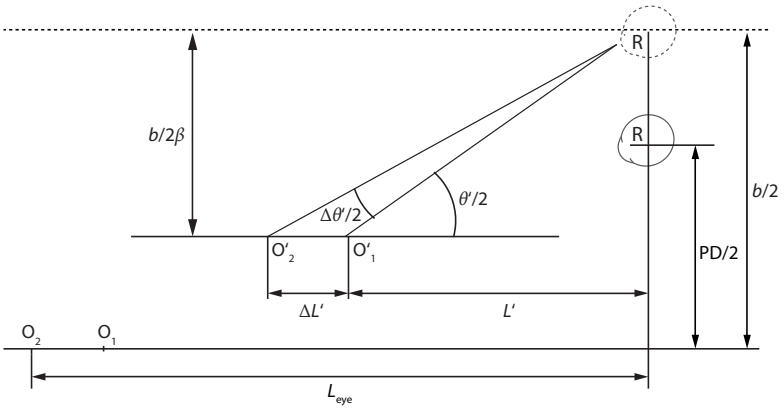

Figure S6.4 Graph to determine the increase of the stereoscopic depth perception when the stereo base b is increased.

the angular magnification of the telescope is given by β, the transverse magnification h_{I}/h_0 equals $1/\beta$.
Thus, any object points O_i in Figure S6.4 are de-magnified by $1/\beta$, which means that the corresponding image points O'_i are located at a distance of $b/2\beta$ from the visual axis of the binocular telescope. Using the geometry in Figure S6.4, we find similar to the procedure for the "naked" eye

$$\theta' = \frac{b}{\beta \cdot L'} \quad \text{and}$$

$$\theta' + \Delta\theta' = \frac{b}{\beta \cdot (L' + \Delta L')} \ .$$

From this, we can easily derive an equivalent formula to Eq. (6.14) (by using the same assumptions), that is,

$$\Delta L' \approx \frac{\beta \cdot \Delta\theta' \cdot L'^2}{b} \ .$$

If we define the stereoscopic magnification Γ_{stereo} as

$$\Gamma_{\mathrm{stereo}} = \Delta\theta'/\varepsilon_{\mathrm{min}}$$

and use the relations

$$L' = \frac{L_{\mathrm{eye}}}{\beta^2} \ \text{ and } \ \Delta L' = \frac{\Delta L_{\mathrm{eye}}}{\beta^2} \ ,$$

we finally obtain

$$\begin{aligned} \frac{\Delta\theta'}{\varepsilon_{\mathrm{min}}} &= \frac{b \cdot \Delta L' \cdot L_{\mathrm{eye}}^2}{\beta \cdot \mathrm{PD} \cdot \Delta L_{\mathrm{eye}} \cdot L'^2} \\ &= \frac{b}{\beta \cdot \mathrm{PD}} \cdot \frac{L_{\mathrm{eye}}^2}{L'^2} \cdot \frac{\Delta L'}{\Delta L_{\mathrm{eye}}} \\ &= \frac{b}{\beta \cdot \mathrm{PD}} \cdot (\beta^2)^2 \cdot \frac{1}{\beta^2} \\ &= \beta \cdot \frac{b}{\mathrm{PD}} \ . \end{aligned} \tag{S6.5}$$

For the given parameters $b = 155\,\mathrm{mm}$, $\mathrm{PD} = 62\,\mathrm{mm}$ and $\beta = 8\times$, we find a stereoscopic magnification of $\Gamma_{\mathrm{stereo}} = 14.8\times$, which is quite noticeable. Compared to the "naked" eye, the stereoscopic vision (stereoscopic depth perception) is improved by a factor of approximately 15.

P6.3
Stereoscopic depth perception

Why is the stereoscopic depth perception an important quantity in microsurgery? Please refer to the diameter of the nerve fibers, blood vessels, and so on. Compare the stereoscopic depth perception of eyes without visual aids and surgical microscopes. Typical parameters of surgical microscopes are $\varepsilon_{\mathrm{min}} = 48.5 \times 10^{-5}$ rad, $b = 26\,\mathrm{mm}$, $f_{\mathrm{obj}} = 200\,\mathrm{mm}$ – $400\,\mathrm{mm}$, $f_{\mathrm{tub}} = 125\,\mathrm{mm}$, $f_{\mathrm{ep}} = 20\,\mathrm{mm}$, and $\Gamma = 0.4$ to 1.

Solution:

The size of blood vessel vary enormously from a diameter of about 25 mm in the aorta to only 8 µm in the capillaries, which allows the red and white blood cells as well as various serum proteins to pass through. Nerve fibers have typical diameters

of $1.5\,\mu$m to $20\,\mu$m. Therefore, for microsurgery, a very good stereoscopic depth perception (i.e., a small value of ΔL_{mic}) is of great importance to allow the surgeon to get a good resolution of microstructures inside the human body. For illustration, we use Eq. (6.15) given by

$$\Delta L_{\mathrm{mic}} = \frac{\varepsilon_{\mathrm{min}} f_{\mathrm{obj}}^2}{b\Gamma(f_{\mathrm{tub}}/f_{\mathrm{ep}}) \pm \varepsilon_{\mathrm{min}} f_{\mathrm{obj}}} \ .$$

Using the data given for the system and Eq. (6.15), we obtain

$$\Delta L_{\mathrm{mic}} = 12 \ldots 119\ \mu\mathrm{m} \ ,$$

depending on the objective's focal length f_{obj} and the zoom magnification Γ.
Again for comparison, the naked eye allows in standard viewing distance a depth resolution of $\Delta L_{\mathrm{eye}} = 45\ \mu$m. With a microscope, we can thus achieve a $4\times$ better depth resolution, again depending on the objective's focal length f_{obj} and the zoom magnification Γ.

P6.4
Achromat design

1. An achromatic lens system shall be designed for the focal length $f = 300\,$mm with crown glass N-FK51A for the (front) positive element and flint glass N-SF6 for the negative element (Table 6.9). The cemented surface should be planar. Calculate the focal lengths and the radii of curvature of the two partial lens elements.
2. How large is the distance of the green ($\lambda = 587\,$nm) from the blue-red ($\lambda = 486\,$nm; $\lambda = 656\,$nm) image plane (secondary chromatic aberration)? How large is the distance between the red and green image plane for a simple lens made of the glass K7? Where does the image for the blue wavelength lie in this case? How large is the relative improvement in the axial chromatic difference overall?
3. Compare the curvatures of the image shell (Section A.1.6.4) for the achromatic lens system and the individual lens element. Which system is more favorable? Why can the achromatic lens system not be flattened with regard to its image shell? Let us use the Rayleigh length $z_{\mathrm{R}} = \lambda/\mathrm{NA}^2$ as a measure for the depth of field. How large may the field angle of the achromatic lens system be in order to obtain a sharply defined image, if the incident bundle is collimated to a diameter of $8\,$mm and only the field curvature is considered?

Solution:

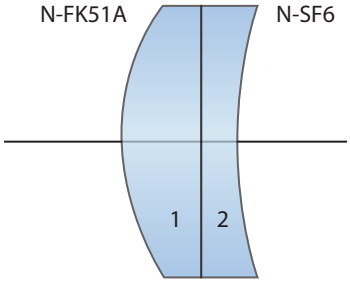

Figure S6.5 Achromatic lens system consisting of a convex N-FK51A lens and a concave N-SF6 lens.

1. For illustration, we use the sketch in Figure S6.5. The total refractive power $\mathcal{D}_{\mathrm{tot}}$ of the cemented system is

$$\mathcal{D}_{\mathrm{tot}} = \mathcal{D}_1 + \mathcal{D}_2 \ . \tag{S6.6}$$

The achromatization condition is given by

$$\frac{\mathcal{D}_1}{\nu_1} + \frac{\mathcal{D}_2}{\nu_2} = 0 \ . \tag{S6.7}$$

Solving these equations yields the individual refractive powers

$$\mathcal{D}_1 = \frac{\mathcal{D}_{\mathrm{tot}}}{1 - \nu_2/\nu_1} = 4.76\ \mathrm{D} \ \Rightarrow f_1 \approx 210\ \mathrm{mm} \ ,$$
$$\mathcal{D}_2 = \frac{\mathcal{D}_{\mathrm{tot}}}{1 - \nu_1/\nu_2} = -1.43\ \mathrm{D} \ \Rightarrow f_2 \approx -699\ \mathrm{mm} \ , \text{where}$$
$$\nu = \frac{n_{\mathrm{e}} - 1}{n_{\mathrm{F}'} - n_{\mathrm{C}'}} \ .$$

The focal length of a lens element with one plane surface is given by Eq. (A12), from which the radius of the lens can be derived as

$$r = f \cdot (n - 1) \ .$$

For the positive lens/front surface, this results in

$$r_1 \approx 210\ \mathrm{mm} \cdot (1.48656 - 1) \approx 100\ \mathrm{mm} \ .$$

For the negative lens/back surface, we have

$$r_2 \approx -699\ \mathrm{mm} \cdot (1.80518 - 1) \approx -563\ \mathrm{mm} \ .$$

It is instructive to calculate the design of the achromat if the lower dispersive crown glass N-FK51A is replaced by a slightly more dispersive K-7 positive element while the higher dispersive flint glass is substituted by the somewhat less dispersive N-KZFS11 negative glass element. The values for a total focal length of 300 mm are

$$\begin{aligned} f_1 &\approx 89\ \text{mm}\ , \\ f_2 &\approx -127\ \text{mm}\ , \\ r_1 &\approx 89\ \text{mm} \cdot (1.51112 - 1) \approx 46\ \text{mm}\ , \end{aligned}$$

and for the negative lens/back surface

$$r_2 \approx -127\ \text{mm} \cdot (1.63775 - 1) \approx -81\ \text{mm}\ .$$

Obviously, the focal lengths and radii are much shorter, which generally leads to higher aberrations (imaging errors).

2. We can calculate the secondary chromatic aberration by starting with the focal length for yellow light with $\lambda = 578$ nm which is $f_{\text{tot}} = 300$ mm. The focal length for red and blue light must be identical in accordance with the achromatization condition. The value is calculated again from Eq. (A12) and follows as

$$\begin{aligned} \frac{1}{f_{\text{red,blue}}} &= \frac{n_{1,656} - 1}{r_1} + \frac{n_{2,656} - 1}{r_2} = 0.00333227\ \text{mm}^{-1} \\ \Rightarrow f_{\text{red,blue}} &= 300.1\ \text{mm}\ . \end{aligned}$$

The difference to f_{tot} is the remaining chromatic aberration, which follows as $\Delta s' = \left| f_{\text{yellow}} - f_{\text{red,blue}} \right| = 100\ \mu\text{m}$.
For an individual plano-convex lens element made of K-7, the secondary spectrum calculation yields

$$\begin{aligned} r &= f \cdot (n_{\text{d}} - 1) = 153.3\ \text{mm}\ , \\ f_{\text{red}} &= \frac{r}{n_{\text{c}} - 1} = 301.5\ \text{mm}\ , \text{ and} \\ f_{\text{blue}} &= \frac{r}{n_{\text{F}} - 1} = 296.6\ \text{mm}\ . \end{aligned}$$

Here, the secondary chromatic aberration is 1.5 mm and -3.4 mm, respectively, that is, it is approximately between $15\times$ and $35\times$ larger.

3. One imaging error of every lens is that the image does not lie in a plane but on a curved shell (field curvature). We can draw the schematic diagram of the curved image shell of an achromat as can be obtained by numerical aberration calculations (see Section A.1.6.4).
The middle image shell lies somewhat further away from the paraxial image plane than the so-called (model) Petzval shell (Figure S6.6), whose radius of curvature

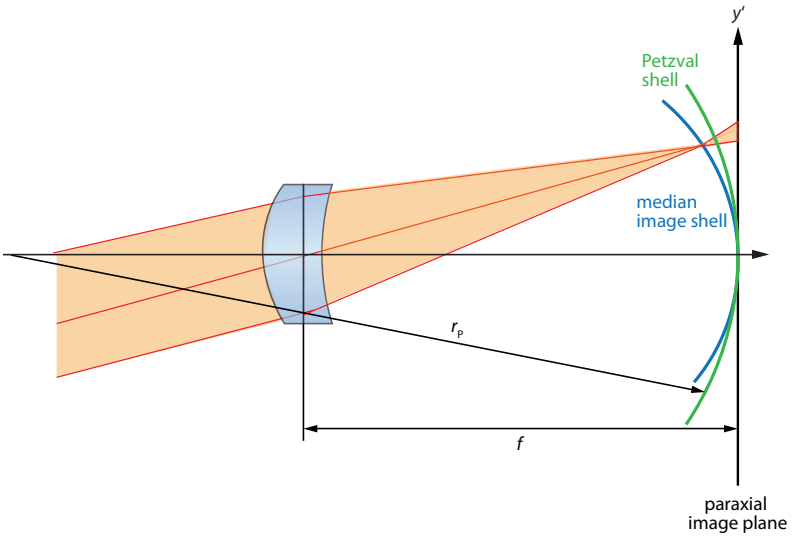

Figure S6.6 Formation of the field curvature imaging error with an achromat.

r_P can be calculated by using aberration theory according to

$$\frac{1}{r_\mathrm{P}} = -\sum_j \frac{1}{n_j f_j} \ . \tag{S6.8}$$

For the individual plano-convex K-7 lens, we obtain for yellow light with a wavelength of 587 nm a radius of curvature of the Petzval shell of

$$r_\mathrm{P} = -453.3 \text{ mm} \ .$$

For the achromat consisting of N-FK51A and N-SF6, the radius of curvature is

$$r_\mathrm{P} = -\left(\frac{1}{312.1 \text{ mm}} + \frac{1}{-1262.3 \text{ mm}}\right)^{-1} = -414.6 \text{ mm} \ .$$

The individual lens and the achromat almost have the same field flattening.
If we want to flatten an achromat, the following condition resulting from rewriting Eq. (S6.8) must be met in addition to Eqs. (S6.6) and (S6.7):

$$\frac{\mathcal{D}_1}{n_1} + \frac{\mathcal{D}_2}{n_2} = 0 \ . \tag{S6.9}$$

This yields the additional condition

$$\frac{\nu_1}{\nu_2} = \frac{n_1}{n_2} \tag{S6.10}$$

to be met by the chosen types of glass. We can easily verify that the condition (S6.10) is not fulfilled for our selected glasses, which means that for these glasses

the field curvature of the achromat cannot be corrected.
When we look at Figure S6.7, at which different glass materials are characterized, condition (S6.10) yields the red lines. Meaningful glass combinations – which are as far apart as possible in order not to make the factor in Eq. (S6.8) too unfavorable – lie between the green boundary curves. A possible solution is given by the blue line or the two glass types of the blue points.

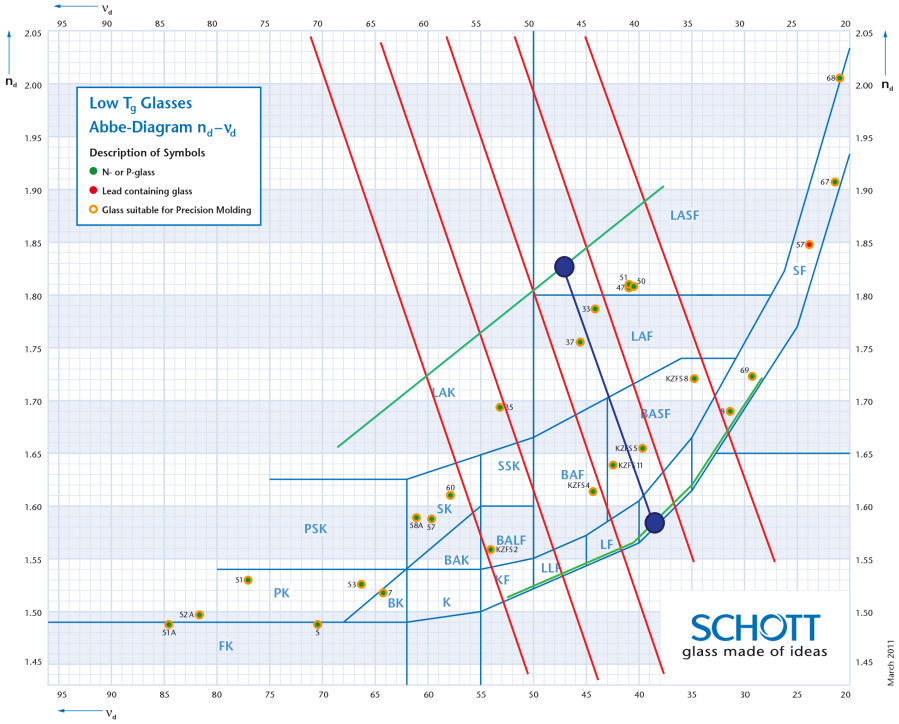

Figure S6.7 Refractive index versus Abbe number for a wavelength of $\lambda = 597\,\text{nm}$ for different types of glass.

If we select a pair of glasses (e.g., glass 1 with $\nu_1 = 44, n_1 = 1.84$, glass 2 with $\nu_2 = 38.5, n_2 = 1.61$), we can verify that the field is almost flat ($r_\text{P} \approx 0$). The design then yields lenses with

$$f_1 \approx 37.5\,\text{mm} \quad \text{and} \quad f_2 \approx -42.9\,\text{mm} \ ,$$

which represent relatively short focal length lenses with other aberration consequences. In general, achromatization and field flatness are thus together not easily achieved with a two-lens system.

Let us finally calculate the maximum field angle that can be allowed by the

achromat to still obtain a sharp image. We start with the numerical aperture of the achromat given by

$$\mathrm{NA} = \sin(u) = \frac{D}{2f} = 0.0133 \ .$$

This yields a depth of field (Section A.2.1.6 and Eq. (6.13)) of

$$\Delta z_{\mathrm{dof}} = \frac{\lambda}{\mathrm{NA}^2} = 3.3 \ \mathrm{mm} \ .$$

At the image height h, the sagitta Δz of the image shell with radius of curvature r_{C} is approximately

$$\Delta z = \frac{h^2}{2r_{\mathrm{C}}} = \Delta z_{\mathrm{dof}} \ .$$

If the radius of curvature is approximately equated to the Petzval radius, this leads to

$$h = \sqrt{2\Delta z_{\mathrm{dof}} \, |r_{\mathrm{P}}|} = 52.3 \ \mathrm{mm} \ .$$

This, in turn, corresponds to a field angle of

$$\begin{aligned} \tan(w) &= \frac{h}{f} = 0.172 \\ \Rightarrow w &\approx 10^{\circ} \ . \end{aligned}$$

P6.5
Apochromat design

Design a three-element apochromat with a focal length of $f = 300\,\mathrm{mm}$. As a third glass N-KZFS11 is available. Compare the resulting performance (regarding chromatic aberration) with the achromat in Problem P6.4 and a single lens made of K-7. For calculation of the secondary spectrum, you can use the $n(\lambda)$ dependence given by the Sellmeier equation

$$n^2(\lambda) - 1 = \frac{B_1 \, \lambda^2}{\lambda^2 - C_1} + \frac{B_2 \, \lambda^2}{\lambda^2 - C_2} + \frac{B_3 \, \lambda^2}{\lambda^2 - C_3} \tag{6.81}$$

with the Sellmeier coefficients B_i and C_i given in Table 6.10.

Solution:

A three-element apochromat system is depicted in Figure S6.8. The total power of this system is given by

$$\mathcal{D}_{\mathrm{tot}} = \sum_{i=1}^{3} \mathcal{D}_i \ , \tag{S6.11}$$

and the achromatization condition by

$$\sum_{i=1}^{3} \frac{\mathcal{D}_i}{\nu_i} = 0 \ . \tag{S6.12}$$

A condition for the disappearance of the secondary spectrum is given by

$$\sum_{i=1}^{3} \frac{P_i \cdot \mathcal{D}_i}{\nu_i} = 0 \ . \tag{S6.13}$$

In the latter condition (S6.13), we used for the so-called partial dispersions of materials

$$P_i(\lambda)_{\lambda,\mathrm{F}} = P_i(\lambda) = \frac{n_i(\lambda) - n_{i,\mathrm{F}}}{n_{i,\mathrm{F}} - n_{i,\mathrm{C}}} \tag{S6.14a}$$

and

$$\nu_{i,\mathrm{d}} = \frac{n_i(587\mathrm{nm}) - 1}{n_i(486\ \mathrm{nm}) - n_i(656\ \mathrm{nm})} = \frac{n_{i,\mathrm{d}} - 1}{n_{i,\mathrm{F}} - n_{i,\mathrm{C}}} \ , \tag{S6.14b}$$

with λ being the third wavelength in addition to λ_F and λ_c to be corrected.

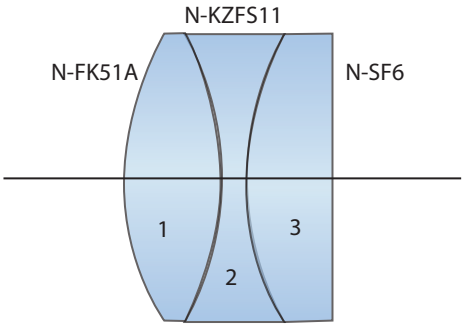

Figure S6.8 Configuration of an apochromatic lens system made of N-FK51A, N-KZFS11, and N-SF6

Table S6.3 Sellmeier coefficients of optical glasses[1)]. Data taken from [9] in Chapter 6.

Type of Glass	B_1	B_2	B_3	C_1	C_2	C_3
N-FK51A	0.971247	0.216901	0.904652	0.004723	0.015358	168.68133
N-SF6	1.779317	0.338150	2.087345	0.013371	0.061753	174.01759
K-7	1.127355	0.124412	0.827101	0.007203	0.026984	100.38459
N-KZFS11	1.332224	0.289242	1.151617	0.008403	0.034424	88.431053

1) C_i are given in $\mu\mathrm{m}^2$, and the wavelength in the Sellmeier equation has to be entered in units of μm.

Equations (S6.11) - (S6.13) can be solved for the individual $\mathcal{D}_i$ via

$$\begin{aligned}\mathcal{D}_1 &= \frac{P_2 - P_3}{P_2 - P_1} \cdot \frac{\nu_1}{T} \cdot \mathcal{D}_{\mathrm{tot}} \\ \mathcal{D}_2 &= \frac{P_3 - P_1}{P_2 - P_1} \cdot \frac{\nu_2}{T} \cdot \mathcal{D}_{\mathrm{tot}} \\ \mathcal{D}_3 &= \frac{P_1 - P_2}{P_2 - P_1} \cdot \frac{\nu_3}{T} \cdot \mathcal{D}_{\mathrm{tot}}\end{aligned} \tag{S6.15}$$

in which

$$T = \frac{\nu_1 \cdot (P_2 - P_1) + \nu_2 \cdot (P_3 - P_1)}{P_2 - P_1} - \nu_3 \ . \tag{S6.16}$$

It is necessary that T has a large value. The value of T can be understood as the "Abbe number" of an artificial glass combined of the materials of the two positive elements (see also [14] in Appendix A).
From Eqs. (S6.15) and (S6.16), we obtain for the third wavelength $\lambda_{\mathrm{g}} = 436\,\mathrm{nm}$ with $P_i(\lambda)_{\lambda,\mathrm{F}} = P_i(\lambda = \lambda_{\mathrm{g}})_{\lambda,\mathrm{F}} = P_{i\mathrm{gF}} = P_i$:

$$\begin{aligned}P_1 &= 0.535824 \ , \\ P_2 &= 0.560442 \ , \\ P_3 &= 0.615699 \ , \\ T &= -77.319 \ .\end{aligned}$$

With this results, we get for the individual lens elements:

$$\begin{aligned}f_1 &= +122.39\ \mathrm{mm} \ , \\ f_2 &= -168.64\ \mathrm{mm} \ , \\ f_3 &= +915.04\ \mathrm{mm} \ .\end{aligned}$$

We start with the first element (N-FK51A) and make it bi-convex; again we assume thin lenses. Then the radii of the first lens element can be calculated to

$$\begin{aligned}R_{c1,\mathrm{front}} &= -R_{c1,\mathrm{back}} = 2f_1 \cdot (n_{1,\mathrm{d}} - 1) = 119.11\ \mathrm{mm} \ , \\ R_{c2,\mathrm{front}} &= R_{c1,\mathrm{back}} = -119.11\ \mathrm{mm} \ , \\ R_{c2,\mathrm{back}} &= -\left(\frac{1}{f_2(n_{2,\mathrm{d}} - 1)} - \frac{1}{R_{c1,\mathrm{back}}}\right)^{-1} = 1109\ \mathrm{mm} \ , \\ R_{c3,\mathrm{front}} &= R_{c2,\mathrm{back}} = 1108.56\ \mathrm{mm} \ , \\ R_{c3,\mathrm{back}} &= -\left(\frac{1}{f_3(n_{3,\mathrm{d}} - 1)} - \frac{1}{r_{c2,\mathrm{back}}}\right)^{-1} = -2196.78\ \mathrm{mm} \ .\end{aligned}$$

As we can see, the second lens (N-KZSF11) will be bi-concave with the second surface being relatively flat, while the third lens (N-SF6) will be again bi-convex with

relatively flat surfaces. This most likely will not be the optimum design for minimum aberrations, but here we just want to illustrate the effect of an apochromatic correction.
With the parameters above, we can calculate the total power of the lens triplet:

$$\mathcal{D}_{\mathrm{tot}}(\lambda) = \sum_{i=1}^{3} \mathcal{D}_i = \sum_{i=3}^{3} (n_i(\lambda) - 1) \cdot \left(\frac{1}{R_{ci,\mathrm{front}}} - \frac{1}{R_{ci,\mathrm{back}}} \right) \quad . \tag{S6.17}$$

This leads to a total focal length of

$$f_{\mathrm{tot}}(\lambda) = \frac{1}{\mathcal{D}_{\mathrm{tot}}(\lambda)} \quad .$$

In Figure S6.9, we plot $\Delta f_{\mathrm{tot}}(\lambda) = f_{\mathrm{tot}}(\lambda) - f_{\mathrm{tot,design}}$. As we can see, the longitudinal chromatic aberration is in the order of a few microns. If we compare this curve

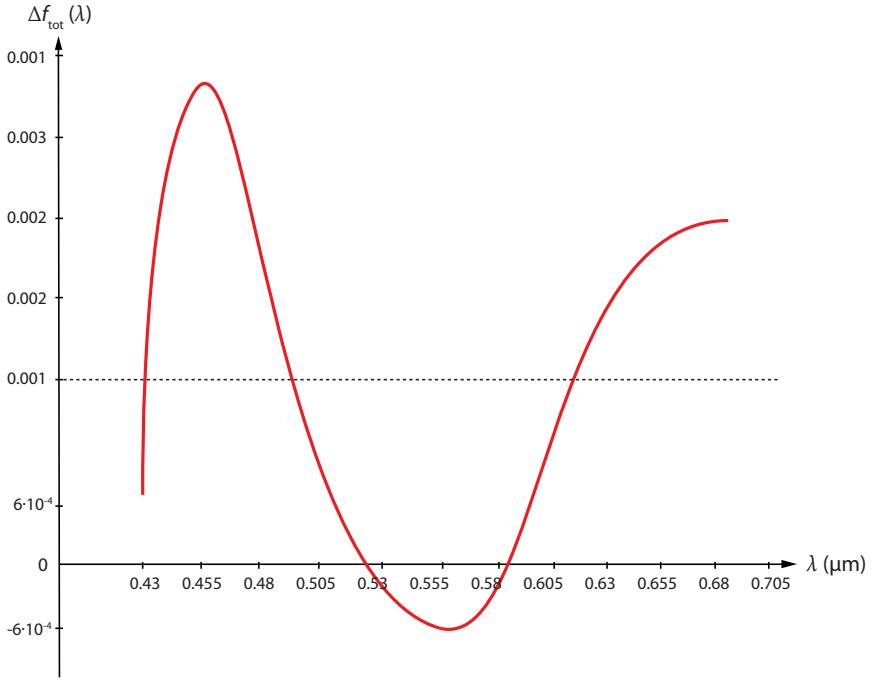

Figure S6.9 Difference of the total focal length $f_{\mathrm{tot}}(\lambda)$ and the designed focal length versus the wavelength λ.

with the results from Problem P6.4 (Figure S6.10), we find indeed a remarkable performance improvement. Please note that in Figure S6.10 the longitudinal chromatic aberration of the apochromat is multiplied by a factor of 100. In reality, it is thus about $100\times$ smaller than an achromat.

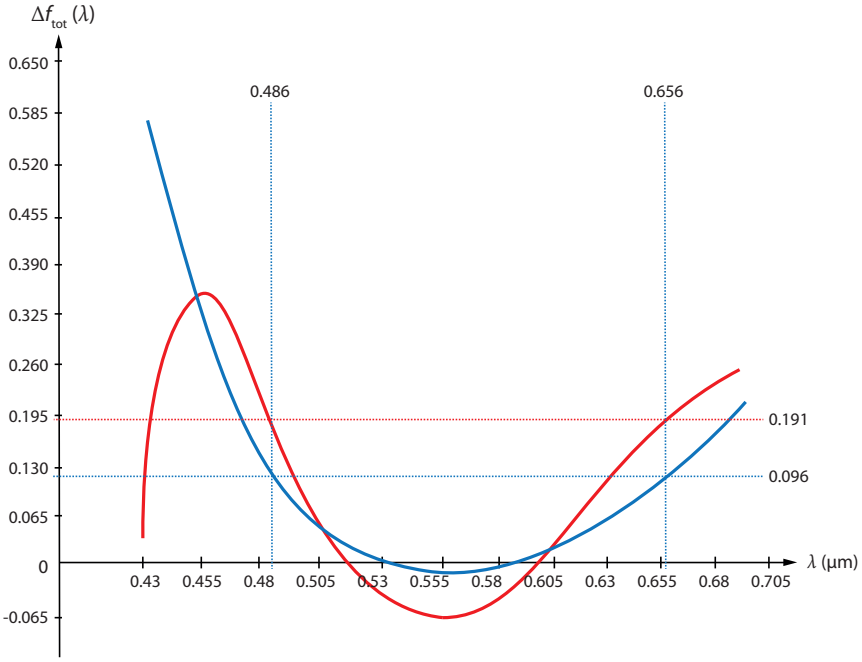

Figure S6.10 Chromatic (longitudinal) aberration. Comparison of $\Delta f_{\mathrm{tot}}(\lambda)$ with the result from Problem P6.4.

P6.6
Varioscope

1. Calculate a simple varioscope (with a negative and a positive lens element) for a working distance range from 200 – 400 mm. Also calculate the related focal lengths. Why should the negative lens component be the front lens?
2. How large is the working distance? What focal lengths do you suggest for the individual lens elements?
3. Can chromatic correction be simultaneously achieved? Select two suitable materials.
4. Calculate the magnification of a surgical microscope for vitro-retinal surgery which uses a wide-angle lens with 125 D and an objective lens with $f_{\mathrm{obj}} = 200$ mm. All other parameters shall be standard. Assume the lens to be located 20 mm above the eye.
   - Where is the intermediate image plane?
   - In order to keep the microscope in a fixed position after insertion of the wide-angle lens, what is the required change of the focal length of the varioscope?
   - How does the situation change, if the lens with 125 D is replaced by a 60 D lens?
5. Calculate for the case of a fundus-imaging microscope the necessary varioscope focal length change (Figure 6.14) when the wide-angle aspheric lens ($\mathcal{D} = +60$ D or $+125$ D) for fundus viewing is placed into the observation path. The working distance of the system should be 200 mm.

Solution:

1. *Approximate solution with $d_{\mathrm{I}} = 0$:*
   In the case of position I with a large working distance, $d = d_{\mathrm{I}} = 0$ approximately applies. With $f_1 > 0$, $f_2 < 0$, and a working distance of $s'_{\mathrm{I}} = 400$ mm, we have

$$\frac{1}{s'_{\mathrm{I}}} = \frac{1}{f_{\mathrm{I}}} = \frac{1}{f_1} + \frac{1}{f_2} \ . \tag{S6.18}$$

   In the case of position II with a working distance of $s'_{\mathrm{II}} = 200$ mm, $d_{\mathrm{II}} + a = f_1$, and the assumption that the focal length f_{II} is approximately 40% longer than the working distance, we have

$$\frac{1}{1.4 s'_{\mathrm{II}}} = \frac{1}{f_{\mathrm{II}}} = \frac{1}{f_1} + \frac{1}{f_2} - \frac{d_{\mathrm{II}}}{f_1 f_2} \ . \tag{S6.19}$$

   The lens equation for imaging through the second element yields (negative lens, virtual image)

$$\frac{1}{s'_{\mathrm{II}}} - \frac{a}{f_1 - d_{\mathrm{II}}} = \frac{1}{f_2} \ , \tag{S6.19}$$

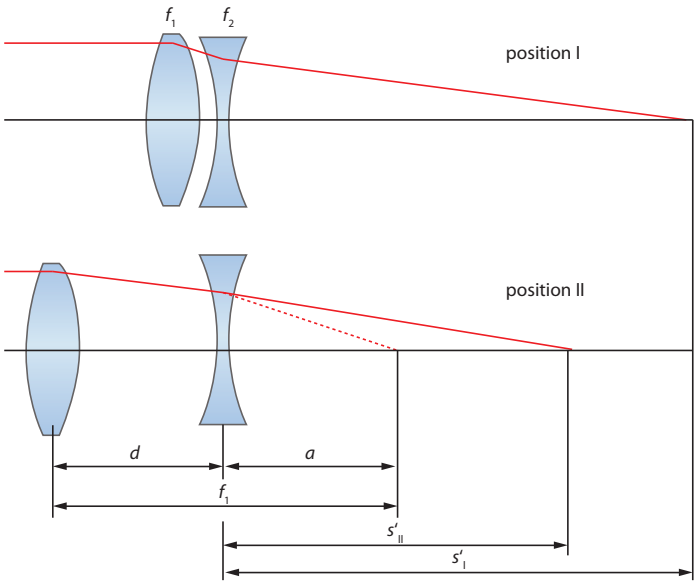

Figure S6.11 Scheme of a varioscope with corresponding geometric parameters.

where

$$\frac{1}{f_2} = \frac{1}{s'_{\mathrm{I}}} - \frac{1}{f_1} \ .$$

Inserted in Eqs. (S6.18) and (S6.19) and f_2 eliminated yields

$$\frac{1}{1.4 s'_{\mathrm{II}}} = \frac{1}{f_1} + \left(1 - \frac{d_{\mathrm{II}}}{f_1}\right)\left(\frac{1}{s'_{\mathrm{I}}} - \frac{1}{f_1}\right) \ ,$$

$$\frac{1}{s'_{\mathrm{II}}} - \frac{1}{f_1 - d_{\mathrm{II}}} = \frac{1}{s'_{\mathrm{I}}} - \frac{1}{f_1} \ .$$

Elimination of d_{II} from both equations leads to a focal length of

$$f_1 = (1.4 - 1)\frac{s'_{\mathrm{I}} s'_{\mathrm{II}}}{s'_{\mathrm{I}} - s'_{\mathrm{II}}} = 160 \text{ mm} \ .$$

From Eq. (S6.19), we obtain

$$f_2 = \frac{f_1 s'_{\mathrm{I}}}{f_1 - s'_{\mathrm{I}}} = -266.7 \text{ mm} \ ,$$

and from Eq. (S6.19) it follows that

$$d_{\mathrm{II}} = f_1 - \frac{f_2 s'_{\mathrm{II}}}{f_2 - s'_{\mathrm{II}}} = 45.714 \text{ mm} \ .$$

From Eqs. (S6.18) and (S6.19), the effective focal lengths follow as

$$f_{\mathrm{I}} = 400\ \mathrm{mm}\ ,$$
$$f_{\mathrm{II}} = 280\ \mathrm{mm}\ .$$

The negative element is the front lens which allows the design of a smaller varioscope size (diameter).

2. *More realistic solution with* $d_{\mathrm{I}} \neq 0$:
In this solution, we have a non-negligible lens thickness in case I and thus a separation of $d_{\mathrm{I}} \neq 0$ between lens 1 and 2. We also assume than the effective focal length is 20% longer that the working distance. As for case II in 1. we find for case I

$$\frac{1}{f_2} = \frac{1}{s'_{\mathrm{I}}} - \frac{1}{f_1 - d_{\mathrm{I}}}\ , \tag{S6.20}$$
$$\frac{1}{1.2s'_{\mathrm{I}}} = \frac{1}{f_{\mathrm{I}}} = \frac{1}{f_1} + \frac{1}{f_2} - \frac{d_{\mathrm{I}}}{f_1 f_2}\ . \tag{S6.21}$$

In case II with d_{II}, we have

$$\frac{1}{f_2} = \frac{1}{s'_{\mathrm{II}}} - \frac{1}{f_1 d_{\mathrm{II}}}\ , \tag{S6.22}$$
$$\frac{1}{1.4s'_{\mathrm{II}}} = \frac{1}{f_{\mathrm{II}}} = \frac{1}{f_1} + \frac{1}{f_2} - \frac{d_{\mathrm{II}}}{f_1 f_2}\ . \tag{S6.23}$$

Equations (S6.20) and (S6.22) yield

$$d_{\mathrm{I}} = f_1 - \frac{f_2 s'_{\mathrm{I}}}{f_2 - s'_{\mathrm{I}}}\ ,$$
$$d_{\mathrm{II}} = f_1 - \frac{f_2 s'_{\mathrm{II}}}{f_2 - s'_{\mathrm{II}}}\ .$$

Accordingly, Eqs. (S6.21) and (S6.23) yield

$$d_{\mathrm{I}} = f_1 + f_2 - \frac{f_1 f_2}{1.2s'_{\mathrm{I}}}\ ,$$
$$d_{\mathrm{II}} = f_1 + f_2 - \frac{f_1 f_2}{1.4s'_{\mathrm{II}}}\ .$$

Elimination of d_{I} and d_{II} leads to

$$f_1 = \frac{1.2 f_2 s'_{\mathrm{I}}}{f_2 - s'_{\mathrm{I}}}\ ,$$
$$f_1 = \frac{1.4 f_2 s'_{\mathrm{II}}}{f_2 - s'_{\mathrm{II}}}\ .$$

From these two equations, we obtain

$$f_2 = \frac{(1.2-1)s'_{\mathrm{I}} s'_{\mathrm{II}}}{1.2s'_{\mathrm{I}} - 1.4s'_{\mathrm{II}}} = -80\ \mathrm{mm}$$

and by re-substitution

$$f_1 = \frac{1.2 f_2 s'_{\mathrm{I}}}{f_2 - s'_{\mathrm{I}}} = 80\ \mathrm{mm}\ .$$

Finally, we get

$$\begin{aligned} d_{\mathrm{I}} &= 13.33\ \mathrm{mm}\ , \\ d_{\mathrm{II}} &= 22.86\ \mathrm{mm}\ , \\ f_{\mathrm{I}} &= 480\ \mathrm{mm}\ , \\ f_{\mathrm{II}} &= 280\ \mathrm{mm}\ . \end{aligned}$$

It is evident that the more realistic solution provides a very different result. The approximation $d_{\mathrm{I}} = 0$ is thus not acceptable at all. Again, the front lens is the negative element. If it were the positive lens, a ray expansion would be obtained at the front lens which would be difficult to correct or would lead to major aberrations. In addition, such a configuration would also make the system bigger in size. In the second example with $d_{\mathrm{I}} \neq 0$, the lenses have to be moved only a much smaller distance $(d_{\mathrm{I}} - d_{\mathrm{II}})$, but also their respective focal lengths.

3. *Chromatic aberration:*
However, the relative displacement of the lens elements changes the heights of the marginal ray (see Appendix A) at the front lens. Thus, the paraxial approximation which we used in the derivation of the cemented achromat is no longer valid. Strictly speaking, simultaneous chromatic correction and varioscope design is not possible. If, however, we set a condition for elements which are not positioned tightly together (as was assumed in the "classic" achromat) such as

$$\frac{\phi_1}{\nu_1} h_1^2 + \frac{\phi_2}{\nu_2} h_2^2 = 0\ ,$$

in which h_1, h_2 are the marginal ray heights, then achromatism is obtained from the following condition

$$\frac{\phi_1}{\nu_1} + \frac{\phi_2}{\nu_2} \cdot \left(\frac{h_2}{h_1}\right)^2 = \frac{\phi_1}{\nu_2} + \frac{\phi_2}{\nu'_2} = 0\ .$$

Here, ν'_2 is the effective Abbe number for material 2. We can derive a condition for ν'_2 which corresponds to the classic achromatism condition

$$\nu'_2 = \nu_2 \left(\frac{h_1}{h_2}\right)^2 = \nu_2 \left(1 - \frac{d}{f_1}\right)^2 > \nu_2$$

and can be easily visualized from Figure S6.11.
If a material with the Abbe number ν'_2 is thus used for the negative front lens (chosen, e.g., for marginal ray heights in the middle position), a considerable reduction of the chromatic aberrations is possible. However, it is advisable to set this corrective position closer to case II with the shorter working distance

and larger numerical aperture, as the depth of field is lower and the longitudinal chromatic aberration is more pronounced in this case. In addition, they have a stronger image quality degrading effect. We leave it to the reader to use the data from Problems P6.4 and P6.5 to determine a suitable glass combination and to calculate the focus for a paraxial ray as a function of the wavelength.

4. *Vitro-retinal surgery with wide-angle lens:*
We assume (in good approximation) that the eye lens images the fundus approximately to infinity. Then, for a fundus imaging lens with $\mathcal{D}_{\mathrm{oph}} = 125\,\mathrm{D}$, we find

$$\frac{1}{s'} = \mathcal{D}_{\mathrm{oph}} \ .$$

Hence, $s' \approx 8\,\mathrm{mm}$, which means that the position of the intermediate plane is positioned about 8 mm after the wide-angle lens (Figure S6.12).
In the case of a fundus imaging lens with $\mathcal{D}_{\mathrm{oph}} = 60\,\mathrm{D}$, we find $s' \approx 16.7\,\mathrm{mm}$.

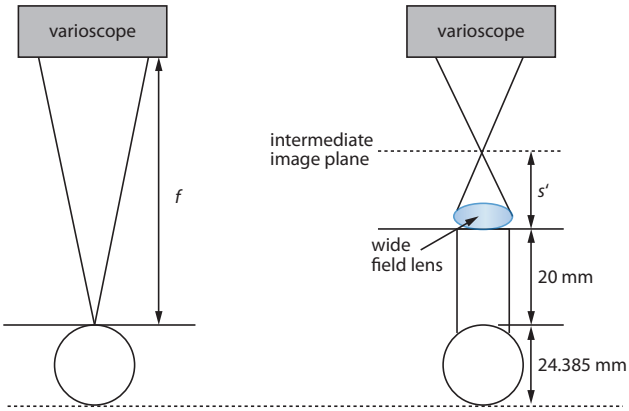

Figure S6.12 Ray diagrams for the optical imaging of a varioscope system.

5. *Focus change in vitro-retinal surgery with a wide-angle lens:*
The change of the focal length of the varioscope is required to transit from a sharp image of the cornea to a sharp image of the fundus. Thus, we have

$$\mathcal{D}_{\mathrm{oph}} = 125\ \mathrm{D} : \Delta f = 20\ \mathrm{mm} + s' = 28\ \mathrm{mm} \ ,$$
$$\mathcal{D}_{\mathrm{oph}} = 60\ \mathrm{D} : \Delta f = 20\ \mathrm{mm} + s' = 36.7\ \mathrm{mm} \ .$$

P6.7
Afocal zoom systems

Let us consider an afocal zoom system, as shown in Figure 6.16, with the focal lengths $f_1 = f_3 = +100$ mm and $f_2 = -20$ mm.

1. What is the condition for afocality in the ABCD matrix notation? What is the matrix of the overall system for a symmetric setup with equal distances? Use this arrangement to calculate the distances for the afocal case. What does the second solution of the equation look like, and why can it not be used here?
2. The zoom system is longest in the symmetrical case. Calculate the system length as a function of the focal lengths? What is the system matrix for the asymmetrical case when decreasing the first distance to $L_1 = 0$. How large is the second distance L_2 and the telescope magnification for this case? What is the general expression used for the overall length L_{tot} here?
3. The zoom factor is generally determined by the ratio of the telescope magnifications from the two end positions. What is the zoom factor M for a symmetrical zoom? What focal lengths should be selected if, for example, a zoom with overall length of $L_{\mathrm{tot}} = 100$ mm and zoom factor $M = 9$ is required?
4. Let us now look at the above zoom system with optical compensation. In this case, only the negative lens L_2 is displaced by z from its center position with distances $L_{\mathrm{s}}/2$. Without the exact compensation, the image plane does not remain exactly constant. To obtain a finite image position, an objective lens with $f_4 = 100$ mm is mounted on the zoom system. Compile the paraxial matrix of the system up to the image plane for arbitrary z values. To simplify the formulas, $f_1 = f_3 = f_4 = f$ should be used here.
   - What is the condition for the image plane in the matrix calculation?
   - What is the expression for the defocussing s' of the image plane?
   - What minimum and maximum values can z technically assume?
   - Plot s' as a function of z.
   - At what interval can the negative element be displaced, if the defocussing is not to be greater than 2 mm?

Solution:

1. The symmetric case is shown in Figure S.13. For the angle behind the system, the general matrix equation yields

$$\theta' = Cx + D\theta \ .$$

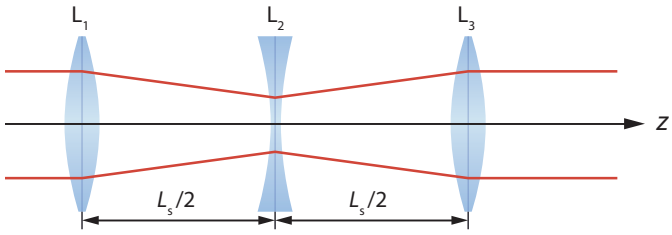

Figure S6.13 Symmetric configuration of a zoom system consisting of three lenses.

A system is afocal if $\theta' = 0$ is valid for all x with $\theta = 0$. This condition is fulfilled for $C = 0$ only. The system's matrix results from

$$\begin{pmatrix} A_\mathrm{s} & B_\mathrm{s} \\ C_\mathrm{s} & D_\mathrm{s} \end{pmatrix} = \begin{pmatrix} 1 & 0 \\ -\mathcal{D}_1 & 1 \end{pmatrix} \cdot \begin{pmatrix} 1 & L_\mathrm{s} \\ 0 & 1 \end{pmatrix} \cdot \begin{pmatrix} 1 & 0 \\ -\mathcal{D}_2 & 1 \end{pmatrix} \cdot \begin{pmatrix} 1 & L_\mathrm{s} \\ 0 & 1 \end{pmatrix} \cdot \begin{pmatrix} 1 & 0 \\ -\mathcal{D}_1 & 1 \end{pmatrix} \ .$$

The elements in detail read

$$\begin{aligned} A_\mathrm{s} &= 1 - L_\mathrm{s}\mathcal{D}_1 - \frac{1}{2}L_\mathrm{s}\mathcal{D}_2 + \frac{1}{4}L_\mathrm{s}^2\mathcal{D}_1\mathcal{D}_2 \ , \\ B_\mathrm{s} &= L_\mathrm{s} - L_\mathrm{s}^2\mathcal{D}_2 \ . \\ C_\mathrm{s} &= -2\mathcal{D}_1 - \mathcal{D}_2 + \frac{1}{2}L_\mathrm{s} \cdot (2\mathcal{D}_1^2 + 2\mathcal{D}_1\mathcal{D}_2) - \frac{1}{4}L_\mathrm{s}^2\mathcal{D}_1^2\mathcal{D}_2 \ , \\ D_\mathrm{s} &= 1 - L_\mathrm{s}\mathcal{D}_1 - \frac{1}{2}L_\mathrm{s}\mathcal{D}_2 + \frac{1}{4}L_\mathrm{s}^2\mathcal{D}_1\mathcal{D}_2 \ . \end{aligned}$$

From $C_\mathrm{m} = 0$, a quadratic equation results for the distance given by

$$\frac{1}{2}L_\mathrm{s} = \frac{\mathcal{D}_1^2 + \mathcal{D}_1\mathcal{D}_2 \pm \mathcal{D}_1^2}{\mathcal{D}_1^2\mathcal{D}_2} \ .$$

The first solution is the relevant one here and delivers

$$\frac{1}{2}L_{\mathrm{s},1} = \frac{2\mathcal{D}_1 + \mathcal{D}_2}{\mathcal{D}_1\mathcal{D}_2} = f_1 + 2f_2 = 60\ \mathrm{mm} \ .$$

The second solution yields $\frac{1}{2}L_{\mathrm{s},2} = f_1$ and has no physical meaning. In this case, the negative middle element is exactly in the focus of the first element and, as a field lens, does therefore not act on the marginal ray. This is a zoom system with image inversion and a long overall length and is thus not desirable.

2. The overall length is twice the distance in the symmetric position (for which the magnification is evidently equal to 1):

$$L_\mathrm{tot} = L_\mathrm{s} = 2f_1 + 4f_2 = 120\ \mathrm{mm} \qquad \text{(S6.24)}$$

In the asymmetrical case with $d_1 = 0$, the system matrix is given by

$$\begin{aligned}\begin{pmatrix} A_{\mathrm{as}} & B_{\mathrm{as}} \\ C_{\mathrm{as}} & D_{\mathrm{as}} \end{pmatrix} &= \begin{pmatrix} 1 & 0 \\ -\mathcal{D}_1 & 1 \end{pmatrix} \cdot \begin{pmatrix} 1 & L_{\mathrm{as}} \\ 0 & 1 \end{pmatrix} \cdot \begin{pmatrix} 1 & 0 \\ -\mathcal{D}_1 - \mathcal{D}_2 & 1 \end{pmatrix} \\ &= \begin{pmatrix} 1 - L_{\mathrm{as}} \cdot (\mathcal{D}_1 + \mathcal{D}_2) & L_{\mathrm{as}} \\ -2\mathcal{D}_1 - \mathcal{D}_2 + L_{\mathrm{as}}\mathcal{D}_1 \cdot (\mathcal{D}_1 + \mathcal{D}_2) & 1 - L_{\mathrm{as}}\mathcal{D}_1 \end{pmatrix} \ .\end{aligned}$$

The afocal case is again obtained for $C_{\mathrm{as}} = 0$ and then yields the distance which equals the overall length

$$L_{\mathrm{as}} = \frac{2f_1 f_2 + f_1^2}{f_1 + f_2} = 75 \text{ mm} \ . \tag{S6.25}$$

Hence, in the symmetrical case, the overall length decreases from 120 mm to 75 mm. In this position, the telescope magnification is

$$\Gamma_{\min} = \frac{\theta'}{\theta} = D_{\mathrm{as}} = 1 - L_{\mathrm{s}}\mathcal{D}_1 = -\frac{f_2}{f_1 + f_2} = 0.25 \ . \tag{S6.26}$$

It can be easily calculated that in the other asymmetrical case (i.e., L_2 with distance 0 to L_3) a magnification of $\Gamma_{\max} = -\frac{f_1+f_2}{f_2} = 4$ results (inverted telescope).

3. With $\Gamma_{\max} = 1/\Gamma_{\min}$ and Eq. (S6.26), the following relation holds for the zoom factor M:

$$M = \frac{\Gamma_{\max}}{\Gamma_{\min}} = \left(\frac{f_1 + f_2}{f_2}\right)^2 = 9 \ .$$

From this equation with $\sqrt{M} = -\left(\frac{f_1+f_2}{f_2}\right)$ and Eq. (S6.24), the focal lengths and the zoom factors as a function of the length $L_{\mathrm{s}} = 100\,\mathrm{mm}$ are obtained via

$$\begin{aligned} f_1 &= \frac{L_{\mathrm{s}}(\sqrt{M}+1)}{2 \cdot (\sqrt{M}-1)} = 100 \text{ mm} \ , \\ f_2 &= -\frac{L_{\mathrm{s}}}{2 \cdot (\sqrt{M}-1)} = -25 \text{ mm} \ . \end{aligned}$$

This results is an asymmetric (minimum) length of the telescope

$$L_{\mathrm{as}} = \frac{2f_1 f_2 + f_1^2}{f_1 + f_2} = 66.7 \text{ mm} \ .$$

The focal lengths can also be determined from the minimum length L_{as} as

$$\begin{aligned} f_1 &= \frac{L_{\mathrm{as}}\sqrt{M}}{\sqrt{M}-1} = 100 \text{ mm} \ , \\ f_2 &= \frac{L_{\mathrm{as}}\sqrt{M}}{1-M} = -25 \text{ mm} \ . \end{aligned}$$

It is instructive for the reader to calculate the position of the lenses L_1 and L_2 as a function of any magnification $\Gamma = \theta'/\theta = D_a$ from the ABCD matrix. To this end, we have to use the following matrix:

$$\begin{pmatrix} A_s & B_s \\ C_s & D_s \end{pmatrix} = \begin{pmatrix} 1 & 0 \\ -\mathcal{D}_1 & 1 \end{pmatrix} \cdot \begin{pmatrix} 1 & L_{23} \\ 0 & 1 \end{pmatrix} \cdot \begin{pmatrix} 1 & 0 \\ -\mathcal{D}_2 & 1 \end{pmatrix} \cdot \begin{pmatrix} a & L_{12} \\ 0 & 1 \end{pmatrix} \cdot \begin{pmatrix} 1 & 0 \\ -\mathcal{D}_1 & 1 \end{pmatrix} \quad , \quad \text{(S6.27)}$$

in which L_{12}, L_{23} are the distances between L_1 and L_2, and L_2 and L_3, respectively. Here, we only provide the result (see also [14] in Appendix A) and advise the reader to plot the distances L_{12} and L_{23} for various Γ according to

$$L_{12}(\Gamma) = \frac{1}{\mathcal{D}_1} \cdot \frac{\Gamma \cdot \Gamma_{max} - 1}{\Gamma \cdot (\Gamma_{max} + 1)} \quad ,$$
$$L_{23}(\Gamma) = \frac{1}{\mathcal{D}_1} \cdot \frac{\Gamma_{max} - \Gamma}{\Gamma_{max} + 1} \quad .$$

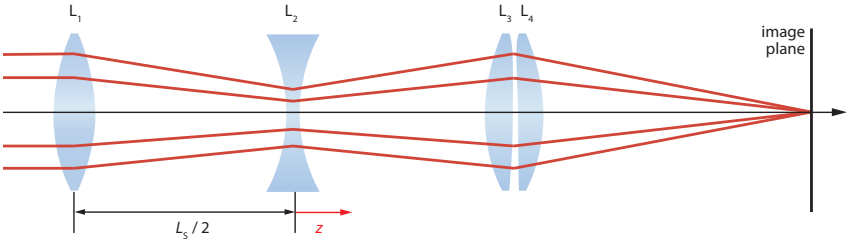

Figure S6.14 Schematic structure of the 4-lens system.

4. The arrangement with an additional objetive lens in shown in Figure S6.14. With $L_s/2 = f + 2f_2$, the system's matrix is determined by

$$\begin{aligned} M &= \begin{pmatrix} 1 & f \\ 0 & 1 \end{pmatrix} \cdot \begin{pmatrix} 1 & 0 \\ \frac{-2}{f} & 1 \end{pmatrix} \cdot \begin{pmatrix} 1 & \frac{L_s}{2} - z \\ 0 & 1 \end{pmatrix} \cdot \begin{pmatrix} 1 & 0 \\ \frac{-1}{f_2} & 1 \end{pmatrix} \cdot \begin{pmatrix} 1 & \frac{L_s}{2} + z \\ 0 & 1 \end{pmatrix} \cdot \begin{pmatrix} 1 & 0 \\ \frac{-1}{f} & 1 \end{pmatrix} \\ &= \begin{pmatrix} -2 + \frac{L_s}{f_2} + \frac{L_s}{f} - \frac{f}{f_2} - \frac{L_s^2}{4f \cdot f_2} - \frac{z^2}{f \cdot f_2} & -L_s + \frac{L_s^2}{4f_2} - \frac{f \cdot L_s}{2f_2} - \frac{z^2}{f_2} - \frac{z \cdot f}{f_2} \\ -\frac{3}{f} - \frac{1}{f_2} + \frac{3L_s}{2f \cdot f_2} - \frac{z}{f \cdot f_2} + \frac{2L_s}{f^2} - \frac{L_s^2}{2f^2 \cdot f_2} + \frac{2z^2}{f^2 \cdot f_2} & 1 + \frac{L_s^2}{2f \cdot f_2} - \frac{L_s}{2f_2} - \frac{2z^2}{f \cdot f_2} - \frac{z}{f_2} \end{pmatrix} \\ &= \begin{pmatrix} \frac{z^2}{f \cdot f_2} & -\frac{z^2}{f_2} - \frac{z \cdot f}{f_2} \\ -\frac{1}{f} - \frac{z}{f \cdot f_2} + \frac{2z^2}{f^2 \cdot f_2} & 7 + \frac{f}{f_2} - \frac{8f_2}{f} - \frac{2z^2}{f \cdot f_2} - \frac{z}{f_2} \end{pmatrix} \quad . \end{aligned} \quad \text{(S6.28)}$$

Here, the condition for the image position results from $x' = 0$ and is valid for all x with $\theta = 0$. Because of

$$x' = Ax + B\theta = Ax \quad ,$$
$$\theta' = Cx + D\theta = Cx \quad ,$$

this means that $A = 0$ must be fulfilled. According to the above expression, this only holds for $z = 0$. The defocussing in the image space results with $\theta = 0$ from

$$s' = \frac{x'}{\theta'} = \frac{A}{C} = \frac{f \cdot z^2}{2z^2 - zf - f \cdot f_2} \quad . \tag{S6.29}$$

$|z|$ cannot be larger than $L_s/2 = 60\,\text{mm}$, as the element would collide with L_3 at this boundary. The defocussing s' as a function of z is plotted in Figure S6.15.

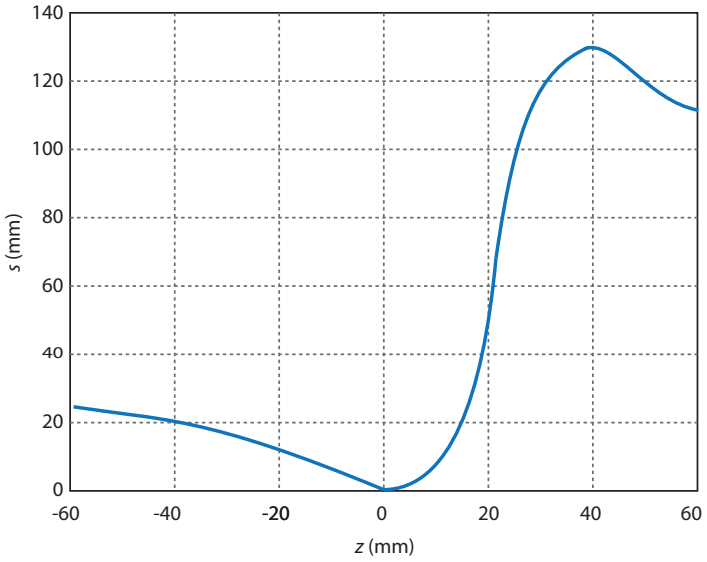

Figure S6.15 The defocussing s' as a function of the displacement of the lens center position z according to Eq. (S6.29).

From Eq. (S6.29) and with $s'_{\max} = 2\,\text{mm}$, we finally obtain

$$z = \frac{s' \cdot f \pm \sqrt{s'^2 f^2 + 4s' f \cdot f_2 \cdot (2s' - f)}}{2 \cdot (2s' - f)} \quad . \tag{S6.30}$$

Through substitution, we find the values $z_{\min} = -7.6\,\text{mm}$ and $z_{\max} = +5.5\,\text{mm}$. This example illustrates how important and effective the displacement of the compensator is for fixating the image plane. From Eq. (S6.28), we can again calculate the necessary displacement of the compensator if we change the matrix element as in Eq. (S6.27), or we allow a compensating behavior of Lens L_4 by providing additional space and movability (change ABCD matrix!).

P6.8
Video documentation

In camera and video documentation the magnification of the surgical microscope is given by

$$\beta_{\mathrm{F}} = \frac{f_{\mathrm{adp}}\,\Gamma}{f_{\mathrm{obj}}} \ , \tag{6.82}$$

where f_{adp} is the focal length of a camera adapter which is generally arranged directly after the zoom system. Typical values lie at around $100\,\mathrm{mm}$.

1. Discuss the meaningfulness of using an HDTV video recorder. The two HDTV-standard image resolutions are 1280×720 pixels and 1920×1080 pixels, in the full format. The width-to-height ratio of the image is $16:9$. The size of CCD image sensors is often specified in inches. Common sizes for professional video cameras are $2/3''$ and $1/2''$. The description of the chip sizes was derived from the external diameter of the old picture tubes. A $1''$ CCD chip has, by definition, the same image diagonal as a $1''$ tube. The length of the image diagonals ($8\,\mathrm{mm}$ for $1/2''$ CCDs) determines the size of the photosensitive surface.
2. How can you increase the depth of field in video documentation? What drawback does this entail?

Solution:

1. The following pixel sizes are obtained for the detectors:

Size	Diagonal (mm)	Side (mm)	Pixel count	Pixel size (μm)
1/2 ”	8	6.97 / 3.92	1280 × 720	5.4
			1920 × 1080	3.6
2/3”	10.67	9.29 / 5.23	1280 × 720	7.2
			1920 × 1080	4.8

We have to understand that the numerical aperture of the objective lens is demagnified by the photo magnification given in Table S6.4. The values result for the numerical aperture of the objective, with the photo magnification

$$\beta_{\mathrm{F}} = \frac{f_{\mathrm{adapter}}}{f_{\mathrm{obj}}} \cdot \Gamma \ , \tag{6.82}$$

objective focal length f_{obj}, the zoom factor Γ, the numerical aperture of the microscope for a given object $\mathrm{NA}_{\mathrm{obj}}$, and the numerical aperture at the camera port $\mathrm{NA}_{\mathrm{F}} = \mathrm{NA}_{\mathrm{obj}}/\beta_{\mathrm{F}}$. Thus, the spatial resolution at the sensor is reduced according to Eqs. (A78) and (6.10) with $f_{\mathrm{adapter}} = 100\,\mathrm{mm}$.

Table S6.4 Typical parameter set of surgical microscopes.

f_{obj} (mm)	Γ	$\mathrm{NA}_{\mathrm{obj}}$	β_{F}	Numerical aperture at the sensor	Optical resolution obtained (µm)	Optical resolution at the sensor (µm)
200	2.5	0.025	1.25	0.020	16.8	16.8
300	2.5	0.017	0.833	0.020	16.8	16.8
400	2.5	0.013	0.625	0.020	16.8	16.8
200	0.4	0.038	0.20	0.19	1.8	1.8
300	0.4	0.025	0.133	0.19	1.8	1.8
400	0.4	0.019	0.10	0.19	1.8	1.8

2. By a comparison with the pixel sizes of the HDTV sensors, it becomes obvious that the numerical aperture and, hence, also the spatial resolution at the sensor only depend on the settings of the zoom magnification and the adapter focal length, but not on the focal length of the objective lens. For higher magnifications, the HDTV sensor resolution is not attained optically. However, HDTV quality is easily achieved for the low and medium magnifications. Therefore, if the zoom range is adjusted, HDTV quality is obtained from about $\Gamma < 0.8\times$ to $1.6\times$ on the choice of sensor for zoom magnifications. The depth of field can be increased by stopping down the adapter aperture of the video system. However, lateral resolution and brightness are lost as a consequence of this.

P6.9
Keratometer

1. Please derive the keratometer equation for the corneal radius of curvature given in Eq. (6.50).
2. The cornea of a patient with a radius of curvature of $r_{\mathrm{C}} = 7.8\,\mathrm{mm}$ is analyzed with a keratometer. The test mires of the keratometer are located at a distance of $30\,\mathrm{cm}$ in front of the corneal vertex. At which distance behind the cornea do we find the reflex images of the mires?
3. We now look at the reflex images with a telescope. The sizes of the reflex images and the original size of the mires shall be equal. How must the telescope magnification be chosen to realize this?

Solution:

1. The keratometer equation can be derived from Eqs. (6.48) and (6.49). Here, we do not consider the usual sign convention, since this is more or less the common

practice in the keratometer literature. In

$$\frac{1}{s'} = \frac{1}{s} + \frac{1}{f'} \ , \tag{6.48}$$

$$\frac{y'}{y} = \frac{s'}{s} \ , \tag{6.49}$$

we use the approximations $y \gg y'$ as well as $s \gg s'$. In addition, we assume the cornea to be a reflecting spherical mirror for which $f' = r_\mathrm{C}/2$. Thus, it follows that

$$\begin{aligned} \frac{1}{s'} \approx \frac{1}{f'} \Rightarrow f' = s' = \frac{r_\mathrm{C}}{2} = \frac{sy'}{y} \\ \Rightarrow r_\mathrm{C} = \frac{2sy'}{y} \ . \end{aligned} \tag{S6.31}$$

Note that $s > 0$ and $s' < 0$ so that $f' < 0$ and $r_\mathrm{C} < 0$. Nevertheless, the radius of curvature r_C is normally specified as a positive value.

2. With $f' = r_\mathrm{C}/2 = 3.9\ \mathrm{mm}$ and $s = 300\ \mathrm{mm}$, we find $s' = 3.85\ \mathrm{mm}$. As a consequence, we observe the reflex images of the mires $3.85\,\mathrm{mm}$ behind the vertex of the cornea.

3. For the corneal system, we have according to Eq. (6.49)

$$\beta = \frac{s'}{s} = 0.0128\times \ .$$

The test mires are de-magnified by the corneal imaging system. As the magnification β' of the telescope system must compensate for this de-magnification, the telescope must provide

$$\beta' = \frac{1}{\beta} = 78\times \ .$$

P6.10
Principle of topometry

Approximate an optical system as a spherical lens with a refractive index of 1.5 and a radius of 25 mm. Then, superimpose on this system a cylindrical optical system with an axis inclined by $30°$ with respect to the vertical line and an additional radius of 85 mm.

1. Calculate (numerical-graphical) a topometric image for an exactly axial alignment. Assume reasonable radii and reasonable stripe distances for the rings of the Placido disk.
2. How does this image change if the optical system is tilted by an angle α?
3. Replace the spherical lens with a parabolic aspherical lens, whereby the radius of curvature of one axis is equal to the radius of the spherical lens. How does the topometric image change?

Solution:

1. The superposition of the spherical surface and the cylindrical surface, rotated by $30°$ in azimuthal direction, yields the following representation for the height topology $z(x, y)$ of the reflecting surface (including both effects):

$$z(x,y) = r_\mathrm{s}\sqrt{1-\left(\frac{x^2+y^2}{r_\mathrm{s}^2}\right)} + r_\mathrm{c}\sqrt{1-\left(\frac{(x\cos\phi + y\sin\phi)^2}{r_\mathrm{c}^2}\right)} \quad . \tag{S6.32}$$

Here, the spherical radius $r_\mathrm{s} = 25$ mm and the cylindric radius $r_\mathrm{c} = 85$ mm, with the latter being effective under an azimuthal angle of ϕ in this case. The terms in the brackets are the coordinates rotated by ϕ. The section in the x, y range of -10 mm to $+10$ mm is considered for the discussion. Figure S6.16 shows the height image as a 3D plot. The astigmatic portion is barely detectable in the height image.

In order to generate the reflected Placido rings, we consider a ring pattern of 10 equidistant rings at a distance of 1.0 mm from each other having a width of 0.2 mm. The generation of the rings is simulated by letting a collimated beam impinge on the surface and recording the reflected light on a projecting screen. This principle is depicted in Figure S6.17.

The image recorded with the camera was generated by superimposing the effect of surface tilt on the incident ring pattern (Figure S6.18, image in the middle). The deflection is modeled by means of the partial derivatives of the function $z(x, y)$. The inclination of the surface $z(x, y)$ (written only for the x component) is given by

$$\tan\alpha' = \frac{\partial z}{\partial x} \quad . \tag{S6.33}$$

Taking into account that negative α' lead to positive deflections 2α, we can use

$$\tan\alpha = \tan(-\alpha') = -\frac{\partial z}{\partial x} \quad . \tag{S6.34}$$

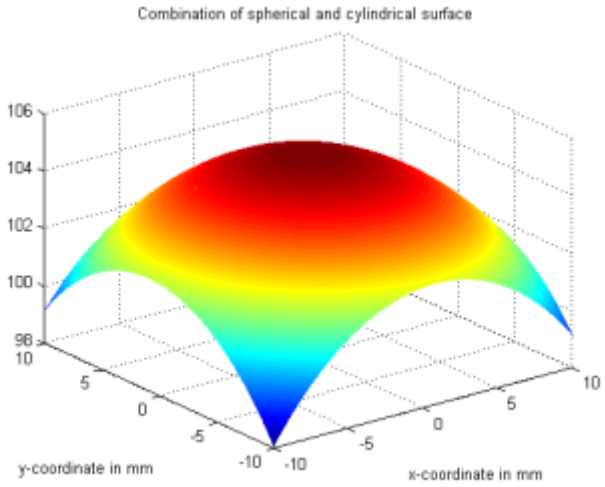

Figure S6.16 Combination of a spherical and cylindric surface shown in a 3D plot.

Therefore, the transversal deflection on the screen is

$$\begin{aligned}\Delta x' &= (s+r-z)\tan(2\alpha) \ , \\ &= (s+r-z)\left(\frac{2\tan\alpha}{1-\tan^2\alpha}\right) \ , \\ &= (s+r-z)\left(\frac{-2\partial z/\partial x}{1-(\partial z/\partial x)^2}\right) \ . \end{aligned} \tag{S6.35}$$

From the representation of the surface according to Eq. (S6.35), the components of the derivative are given by

$$\frac{\partial z}{\partial x} = -\frac{x}{\sqrt{r_s^2-(x^2+y^2)}} - \frac{\cos\phi\cdot(x\cos\phi+y\sin\phi)}{\sqrt{r_c^2-(x\cos\phi+y\sin\phi)^2}} \ , \tag{S6.36}$$

$$\frac{\partial z}{\partial y} = -\frac{y}{\sqrt{r_s^2-(x^2+y^2)}} - \frac{\sin\phi\cdot(x\cos\phi+y\sin\phi)}{\sqrt{r_c^2-(x\cos\phi+y\sin\phi)^2}} \ , \tag{S6.37}$$

such that the following transformation is obtained for the camera image using an arbitrary scaling factor (depends on the imaging relationships of the camera):

$$x' = x + \Delta x' \ , \quad y' = y + \Delta y' \ . \tag{S6.38}$$

Substituting Eqs. (S6.35), (S6.36), and (S6.37) into (S6.38) yields a rule for computing the simulation of the signal given by

$$x' = x - 2s\left(1+\frac{r-z}{s}\right)\cdot\frac{\partial z/\partial x}{1-(\partial z/\partial x)^2} \ , \tag{S6.39}$$

$$y' = y - 2s\left(1+\frac{r-z}{s}\right)\cdot\frac{\partial z/\partial y}{1-(\partial z/\partial y)^2} \ . \tag{S6.40}$$

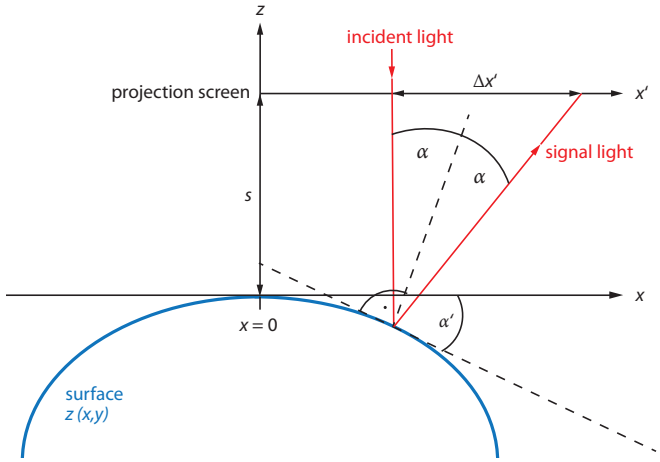

Figure S6.17 Geometry of a collimated incident light beam which is reflected to a projection screen.

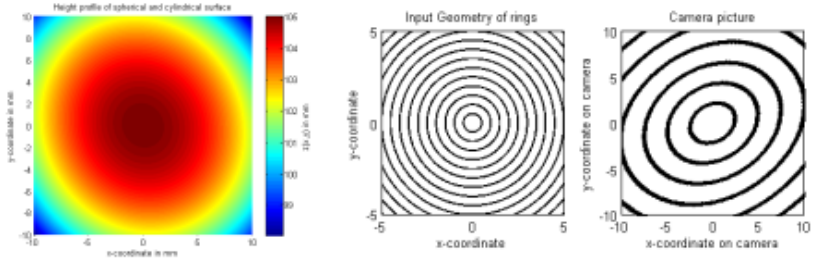

Figure S6.18 Numerically calculated height levels of a surface (left), the input geometry of rings (middle), and the resulting camera image of the rings (right).

In practical applications, it is often possible to use the approximations $r - z \ll s$. This simplifies Eqs. (S6.39) and (S6.40) to

$$x' = x - 2s \cdot \frac{\partial z/\partial x}{1 - (\partial z/\partial x)^2} \quad , \tag{S6.41}$$

$$y' = y - 2s \cdot \frac{\partial z/\partial y}{1 - (\partial z/\partial y)^2} \quad . \tag{S6.42}$$

Figure S6.18 shows the numerically calculated levels of the surface (left), the input geometry of the rings (middle), and the camera image of the rings (right). It is evident that the astigmatic portion leads to the marked elliptical deformation of the rings. The spherical curvature portion causes the originally equidistant rings to become non-equidistant. The distances between the rings become larger further out, that is, for larger x, y values. Obviously, the topometry is much more

sensitive to changes of the surface (curvatures) than the height measurement. This is due to the fact that the topometry is based on the derivatives of the surface. The derivative defines the angle of inclination of the surface with respect to the incident beam. According to the law of reflection, this is crucial for beam deflection.

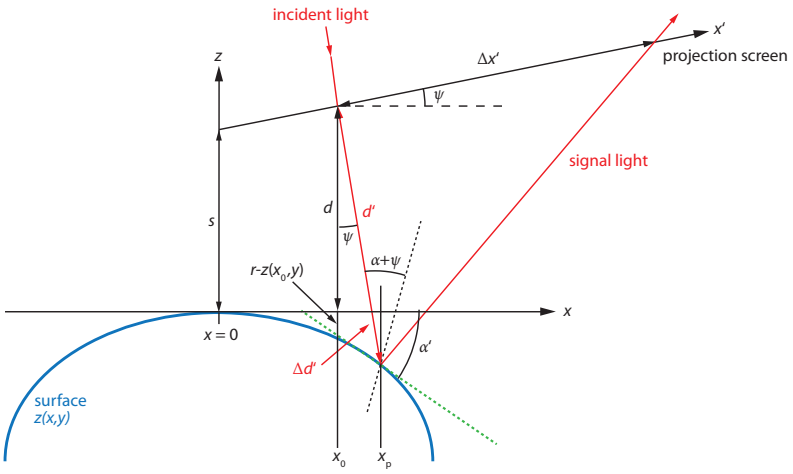

Figure S6.19 Topometric geometry for a tilted system against the optical axis of the lens (angles are exaggerated for clarity).

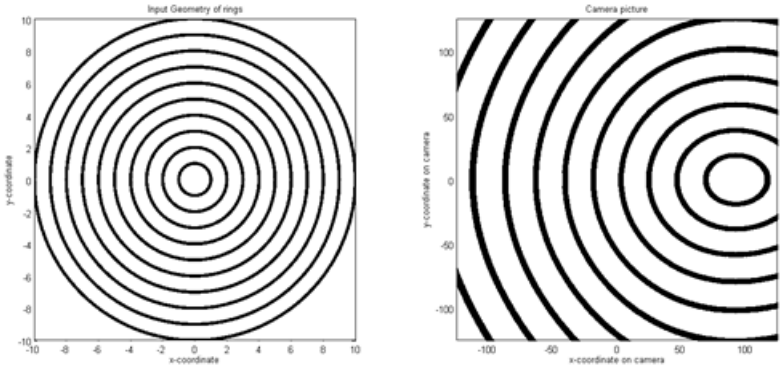

Figure S6.20 Ring pattern for a tilted topometry geometry.

2. Tilting by $\psi = 10^\circ$ in x direction around the y-axis leads to a somewhat more complicated geometry. From the geometry in Figure S6.19, we can derive

$$\Delta x' = d' \tan(2(\alpha + \psi))$$

with $\tan\alpha = -\frac{\partial z}{\partial x}$ at $x = x_\mathrm{p}$. Furthermore, we have

$$\begin{aligned} d &= s + (r - z(x_0, y) + x_0 \cdot \tan\psi) \ , \\ \cos\psi &= \frac{d}{d' - \Delta d'} \approx \frac{d}{d'} \ , \\ x_\mathrm{p} &\approx x_0 + d' \sin\psi \ , \\ x_0 &= x_0' \cos\psi \\ \Rightarrow x_\mathrm{p} &\approx x_0' \cos\psi + d \tan\psi \ . \end{aligned}$$

We use again the identities

$$\begin{aligned} \tan(2(\alpha+\psi)) &= \frac{2\tan(\alpha+\psi)}{1-\tan^2(\alpha+\psi)} \ , \\ \tan(\alpha+\psi) &= \frac{\tan(\psi)+\tan(\alpha)}{1-\tan(\alpha)\cdot\tan(\psi)} \end{aligned}$$

and obtain for the deflection

$$\Delta x' = \frac{2d}{\cos\psi} \cdot \frac{\tan(\psi)+\tan(\alpha)}{1-\tan(\alpha)\cdot\tan(\psi)} \cdot \frac{1}{1-\left(\frac{\tan(\psi)+\tan(\alpha)}{1-\tan(\alpha)\cdot\tan(\psi)}\right)^2} \ , \qquad \text{(S6.43)}$$

with $d = s + (r - z(x_0' \cos\psi, y) + x_0' \sin\psi)$, $\tan\alpha = -\partial z/\partial x$ at $x = x_\mathrm{p}$, and $x_\mathrm{p} = x_0' \cos\psi + d\tan\psi$. It should be noted that x_0' is the x-position of the impinging beam in the camera plane, x_p the corresponding x-coordinate of the point of reflection on the surface, and $\Delta x'$ the deflection as measured in the (tilted) camera plane. As we can see from Figure S6.20, the rings and the center of the pattern are shifted. The distances become considerally more one-sided in x direction.

3. If a parabolic rotationally-symmetric portion with an identical summit osculating radius r_s is present, the shape of the surface is given by

$$z(x,y) = \frac{x^2+y^2}{2r_\mathrm{p}} + r_\mathrm{c}\sqrt{1-\left(\frac{(x\cos\phi + y\sin\phi)^2}{r_\mathrm{c}^2}\right)} \qquad \text{(S6.44)}$$

and the derivatives by

$$\begin{aligned} \frac{\partial z}{\partial x} &= -\frac{x}{r_\mathrm{p}} - \frac{\cos\phi\cdot(x\cos\phi + y\sin\phi)}{\sqrt{r_\mathrm{c}^2 - (x\cos\phi + y\sin\phi)^2}} \\ \frac{\partial z}{\partial y} &= -\frac{y}{r_\mathrm{p}} - \frac{\sin\phi\cdot(x\cos\phi + y\sin\phi)}{\sqrt{r_\mathrm{c}^2 - (x\cos\phi + y\sin\phi)^2}} \ . \end{aligned} \qquad \text{(S6.45)}$$

Figure S6.21a shows the surface relief and ring geometry for this case ($r_\mathrm{c} \to \infty$). The significant difference as compared to the spherical surface is that the rotationally-symmetrical portion generates equidistant rings further out than in the spherical case.

Figure S6.21b depicts the surface relief and ring geometry for a "different surface" of parabolic and a spherical surface to equal radii. This shows again the sensitivity of the topometry/deflection measurement.
It is instructive to calculate the deflected ring position as a function of the incoming position for both surfaces (with the assumption that $r_\mathrm{s} = r_\mathrm{p} = r$). It is sufficient to do this for the x coordinate. We start for the sphere from Eq. (S6.42b), where we had

$$x' = x - 2s\left(1 + \frac{r-z}{s}\right) \cdot \frac{\partial z/\partial x}{1-(\partial z/\partial x)^2} \ ,$$
$$\frac{\partial z}{\partial x} = -\frac{x/r}{\sqrt{1-(x^2/r^2)}} = -\frac{\beta}{\sqrt{1-\beta^2}}$$

in which $\beta = x/r$. Thus, we can write

$$x' = x + 2s\left(1 + \frac{r-z}{s}\right)\left(\frac{\frac{\beta}{\sqrt{1-\beta^2}}}{1-\left(\frac{\beta}{\sqrt{1-\beta^2}}\right)^2}\right) \ .$$

With $z = r\sqrt{1-\beta^2}$, we obtain

$$\frac{x'}{r} = \beta' = \beta + 2\frac{s}{r}\left(1 + \frac{r\cdot(1-\sqrt{1-\beta^2}}{s}\right)\left(\frac{\frac{\beta}{\sqrt{1-\beta^2}}}{1-\left(\frac{\beta}{\sqrt{1-\beta^2}}\right)^2}\right) \ .$$

For the parabola, we start from Eq. (S6.44b), where

$$x' = x + 2s\left(1 + \frac{r-z}{s}\right) \cdot \frac{\partial z/\partial x}{1-(\partial z/\partial x)^2} \ ,$$
$$\frac{\partial z}{\partial x} = -\frac{x}{r} = -\beta \ .$$

Thus, we can write

$$x' = x + 2s\left(1 + \frac{r-z}{s}\right)\left(\frac{\beta}{1-\beta^2}\right) \ .$$

With $z = r(1 - \frac{1}{2}\beta^2)$, we obtain

$$\frac{x'}{r} = \beta' = \beta + 2\frac{s}{r}\left(1 + \frac{r\beta^2}{2s}\right) \cdot \frac{\beta}{1-\beta^2} \ .$$

Figure S6.22 shows the deflected ring position as a function of the incoming position for both surfaces. Obviously, for small positions (close to the axis) and for both surfaces, we obtain equidistant reflected rings. The spherical surface "departs" much faster from this picture with equidistant rings.

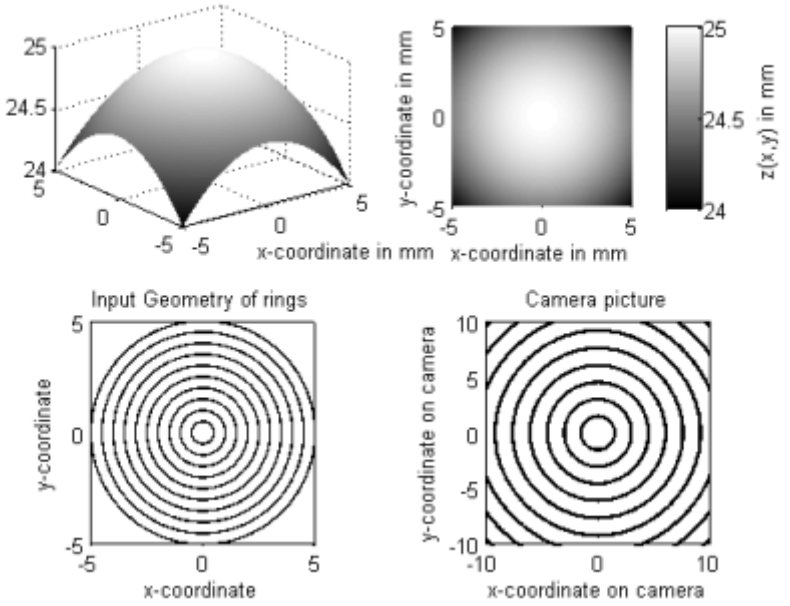

Figure S6.21a "Placido-like" plot of a parabolic surface.

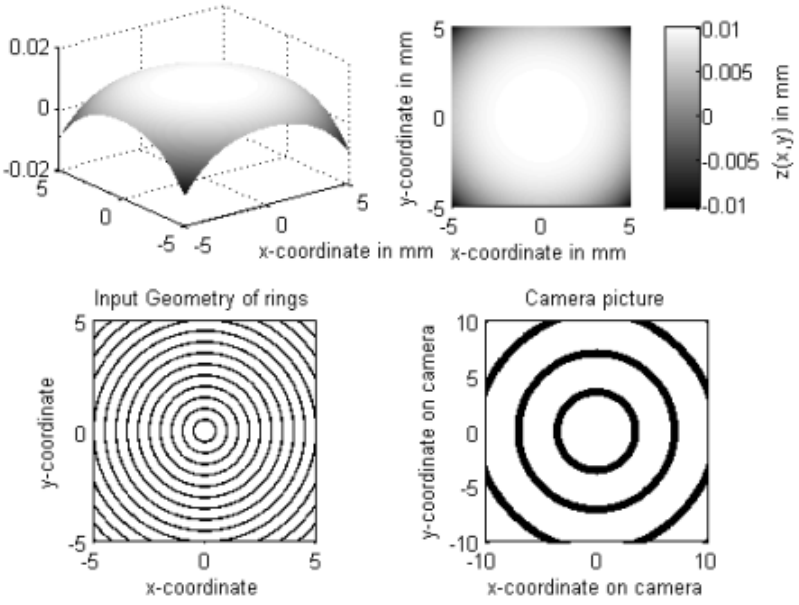

Figure S6.21b "Difference plots" between a spherical and a parabolic surface of equal radii.

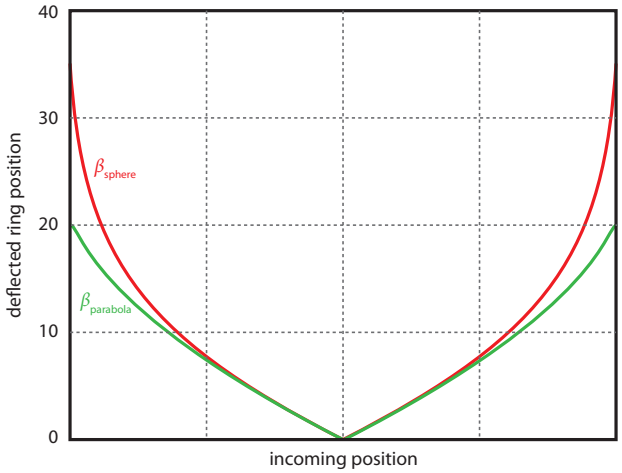

Figure S6.22 “Camera ring position” as a function of incoming ring radius.

P6.11
Slit lamp

1. As an alternative to a telescopic system, we can also implement a Greenough miscroscope to the observation path of a slit lamp. The total magnification of the Greenough miscroscope is given by the product of the magnification of the objective lens β_{obj} and the magnification of the eyepieces β_{ep}. Show that the magnification of the objective lens is given by $\beta_{\mathrm{obj}} = L_{\mathrm{tub}}/f_{\mathrm{obj}}$, where L_{tub} denotes the optical tube length.
2. Slit lamp microscopes usually have a numerical aperture of $\mathrm{NA} = 0.05$. Let us assume that imaging aperture and illumination aperture are equal. Calculate the microscope resolution for a wavelength of $\lambda = 550\,\mathrm{nm}$. Calculate the minimum and maximum usable magnifications $\beta_{\mathrm{um,min}}$ and $\beta_{\mathrm{um,max}}$, respectively (Section 6.2.2). Discuss the result with reference to typical magnifications used in slit lamp microscopes.

Solution:

1. The lateral magnification is given by

$$\beta_{\mathrm{obj}} = -\frac{s'}{s} \quad .$$

With the paraxial imaging equation (A14), we have

$$\frac{1}{s'} - \frac{1}{s} = \frac{1}{f_{\mathrm{obj}}} \quad .$$

Consequently, we obtain

$$\begin{aligned} \beta_{\mathrm{obj}} &= s' \left(\frac{1}{f_{\mathrm{obj}}} - \frac{1}{s'} \right) \\ &= \frac{s'}{f_{\mathrm{obj}}} - 1 \\ &= \frac{s' - f_{\mathrm{obj}}}{f_{\mathrm{obj}}} \quad . \end{aligned}$$

Since the optical tube length is $L_{\mathrm{tub}} = s' - f_{\mathrm{obj}}$, it follows that

$$\beta_{\mathrm{obj}} = \frac{L_{\mathrm{tub}}}{f_{\mathrm{obj}}} \quad .$$

According to Eq. (6.8), the lateral spatial resolution of a microscope is determined by

$$\Delta(x,y)_{\mathrm{mic}} = \frac{1.22\lambda}{\mathrm{NA}_{\mathrm{mic}} + \mathrm{NA}_{\mathrm{c}}} \quad .$$

λ denotes the wavelength of the illuminating light and $\mathrm{NA_{mic}}$ the numerical aperture of the microscope. With $\mathrm{NA_{mic}} = \mathrm{NA_c} = 0.05$ and $\lambda = 550\,\mathrm{nm} = 0.55\,\mu\mathrm{m}$, we get

$$\Delta(x,y)_{\mathrm{mic}} = 0.61\,\frac{0.55}{0.05} = 7\ \mu\mathrm{m}\ .$$

The lateral spatial resolution of the microscope is approximately 7 µm.

2. According to Eq. (6.12), the range of usable magnification is given by

$$500\ \mathrm{NA_{mic}} \leq \beta_{\mathrm{um}} \leq 1000\ \mathrm{NA_{mic}}\ .$$

With $\mathrm{NA} = 0.05$, we find

$$\beta_{\mathrm{um,min}} = 25\times \text{ and } \beta_{\mathrm{um,max}} = 50\times\ .$$

The magnification normally used in slit lamp microscopes are in range of $10\times$ to $25\times$. At values below $25\times$, the theoretically possible resolution of the microscope is not exhausted – in favor of greater brightness of the image.

P6.12
Scheimpflug principle

Imagine yourself standing in front of the highest church tower in Europe with your medium-format camera (6 cm × 6 cm) in hand. The market square in front of the tower allows you to be at a distance of 100 m from the foot of the tower. You have two objective lenses with focal lengths of $f_1 = 50$ mm and $f_2 = 85$ mm to choose from. The F-number of the objective lenses is $f_i/d_{\mathrm{pupil}} = 1.4$ in each case; with the diameter of the entrance pupil d_{pupil}. You also have a bellow device which allows you to tilt the camera objective lens with respect to the film plane. Select the optimal arrangement allowing the church tower to be image-filling and in sharp focus, if possible, along its entire height.

Solution:

The parameters, $h = 161$ m (object height of church tower, "Ulmer Muenster"), $s_{\mathrm{u}} = 100$ m (distance from foot point), f, and h' (size of the film format) are shown in Figure S6.23a. It must be noted that, in the film diagonal, $h' = 6$ cm or $h' = \sqrt{2}\cdot 6\,\mathrm{cm} = 8.48$ cm must be used, depending on the azimuth rotation of the camera. This rotation of the film format along with the camera is schematically shown in Figure S6.23b. The rotation can be used to align the church tower along the diagonal of the film format which allows for a gain of 41% in length.
As an additional condition, the church tower of height h is perpendicular to the distance line s_{u}. This is for instance not exactly true in the case of the tower of Pisa and

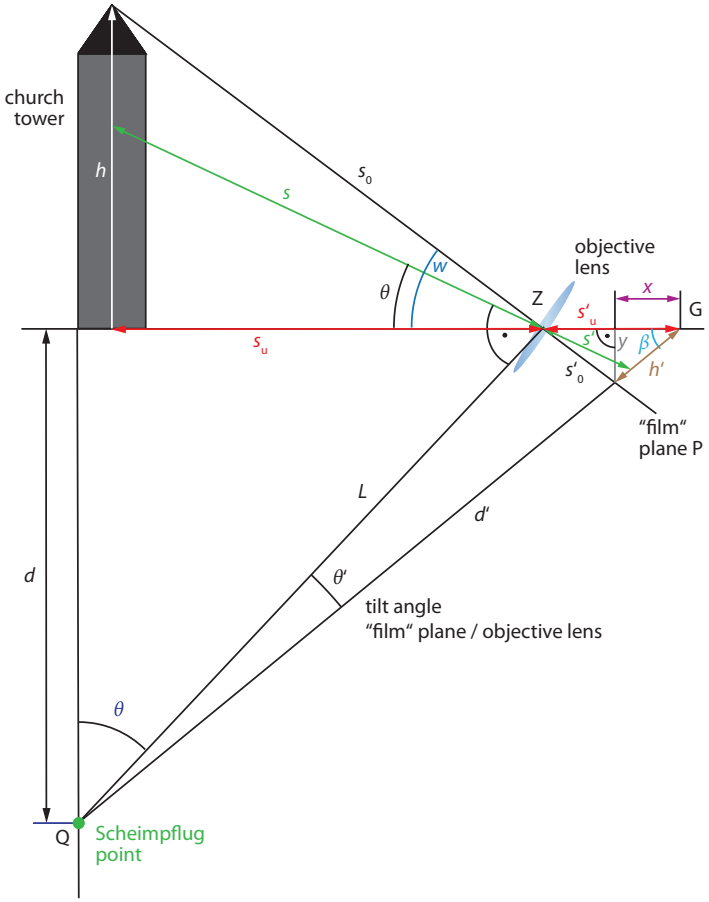

Figure S6.23a Scheimpflug arrangement to photograph a church tower.

then depends on from which side the image is taken.
The selected parameter in these considerations is the angle of inclination θ of the objective lens axis with respect to the horizontal line. The following consideration consists of calculating the maximal height of the object that can be imaged on the film (either on 6 cm or on 8.48 cm edge length) as a function of the angle of inclination while taking the secondary condition of the tilt angle θ' into account.
The following geometric relationships are evident from Figure S6.23a:

- Object focal intercept along the tilted camera axis:

$$s = \frac{s_\mathrm{u}}{\cos\theta}$$

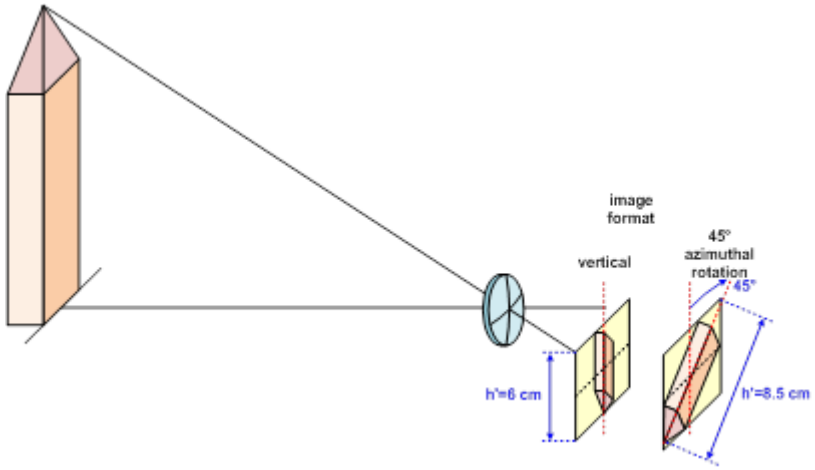

Figure S6.23b Rotation of the format to fill the entire film plane.

- Distance of the point of intersection Q of the main plane and object planes:

$$L = \frac{s_\mathrm{u}}{\sin\theta} \quad .$$

- Lens equation with all distances being considered positive (real image):

$$\frac{1}{f'} = \frac{1}{s'} + \frac{1}{s}$$
$$\Rightarrow s' = \frac{f' \cdot s}{s - f'} = \frac{f \cdot s_\mathrm{u}}{s_\mathrm{u} - f \cdot \cos\theta} \quad .$$

The tilt angle θ' of the film plane with respect to the main plane of the objective lens as a function of the angle on inclination θ is given by

$$\tan\theta' = \frac{s'}{L} = \frac{\sin\theta}{s_\mathrm{u}} \cdot \frac{f' \cdot s_\mathrm{u}}{s_\mathrm{u} - f' \cdot \cos\theta} = \frac{f' \cdot \sin\theta}{s_\mathrm{u} - f' \cdot \cos\theta} \quad . \tag{S6.46}$$

The distance s'_u can be calculated by means of an auxiliary distance d via

$$d = \frac{s_\mathrm{u}}{\tan\theta} = \frac{s_\mathrm{u} + s'_\mathrm{u}}{\tan(\theta + \theta')} \quad ,$$
$$s'_\mathrm{u} = s_\mathrm{u} \cdot \left(\frac{\tan(\theta + \theta')}{\tan\theta} - 1 \right) \quad . \tag{S6.47}$$

The field angle w is determined by

$$\cot w = \frac{s_\mathrm{u}}{h} \quad . \tag{S6.48}$$

Using the auxiliary angle

$$\begin{aligned}\beta &= 90^\circ - (\theta + \theta') \ , \\ \cos\beta &= \sin(\theta + \theta') \ , \\ \sin\beta &= \cos(\theta + \theta') \ ,\end{aligned}$$

and considering the triangle PGZ with an auxiliary distance y that is perpendicular to s'_u and distance x leads to

$$\begin{aligned}y &= (s'_\mathrm{u} - x)\tan w = x \cdot \tan\beta \ , \\ x &= s'_\mathrm{u} \cdot \frac{\tan w}{\tan w + \tan\beta} \ .\end{aligned}$$

Accordingly, the image height is

$$\begin{aligned}h' &= \frac{x}{\cos\beta} = \frac{s'_\mathrm{u}}{\cos\beta} \cdot \frac{\tan w}{\tan w + \tan\beta} = \frac{s'_\mathrm{u}}{\cos\beta + \cot w \cdot \sin\beta} \\ &= \frac{s_\mathrm{u}}{\sin(\theta + \theta') + \cot w \cdot \cos(\theta + \theta')} \ .\end{aligned}$$

Substituting Eqs. (S6.46) and (S6.47) yields

$$h' = \frac{s_\mathrm{u}}{\sin(\theta + \theta') + s_\mathrm{u}/h \cdot \cos(\theta + \theta')} \cdot \left(\frac{\tan(\theta + \theta')}{\tan\theta} - 1 \right) ,$$

and resolving with respect to h finally leads to

$$h = \frac{s_\mathrm{u} \cdot \cos(\theta + \theta')}{s_\mathrm{u}/h' \cdot (\cot\theta \cdot \tan(\theta + \theta') - 1) - \sin(\theta + \theta')} \ . \tag{S6.49}$$

Varying the angle θ, using Eq. (S6.46) to calculate the angle θ' and Eq. (S6.49) to calculate the maximal attainable object height, the behavior for both focal lengths in the case of the diagonal format with $h' = 8.48\,\mathrm{cm}$ is illustrated in Figure S6.24a.
The maximal possible object height for the objective lens with $f' = 85\,\mathrm{mm}$ is $132\,\mathrm{m}$, which is not enough for the Ulmer Muenster (161 m). Evidently, using the objective lens with $f' = 50\,\mathrm{mm}$ in the 45° azimuth angle position allows full imaging of the object at $\theta = 59.92^\circ$. This is based on the assumption that the width of the church tower is negligibly small. The additional required inclination of the film plane is $\theta' = 0.0248^\circ$. This value is very small and considering the finite depth of field of the image, this tilting could be omitted.
If the azimuthal rotation is omitted in order to cover the entire base of the church, $h' = 6\,\mathrm{cm}$ must be used. This leads to the curves shown in Figure S6.24b. Again, there is no chance to cover the object completely using the objective lens with $f = 85\,\mathrm{cm}$. Two solutions are obtained for the objective lens with $f' = 50\,\mathrm{mm}$, that is for the angles

$$\theta = 15.42^\circ, \ \ \theta' = 0.0076^\circ \ ,$$

and

$$\theta = 42.70^\circ, \ \ \theta' = 0.0194^\circ \ .$$

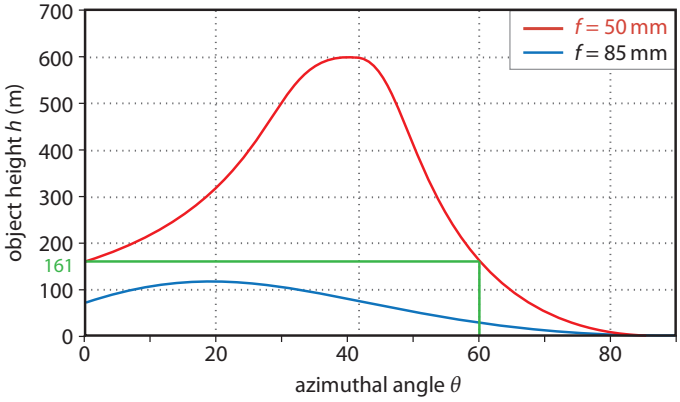

Figure S6.24a Object height h versus the angle of inclination θ for two focal lengths $f = 50$ mm and $f = 85$ mm and for a diagonal format with $h' = 8.48$ cm.

Actually, using the diagonal format is not particularly reasonable. It becomes obvious from the real relationships that the width of the Ulmer Muenster at its base is not negligible (Figure S6.24c). Because of the distortion typically observed for Scheimpflug setups, the object appears to have a width of 108 m, meaning that a square format is also filled by 67% in its other dimension.

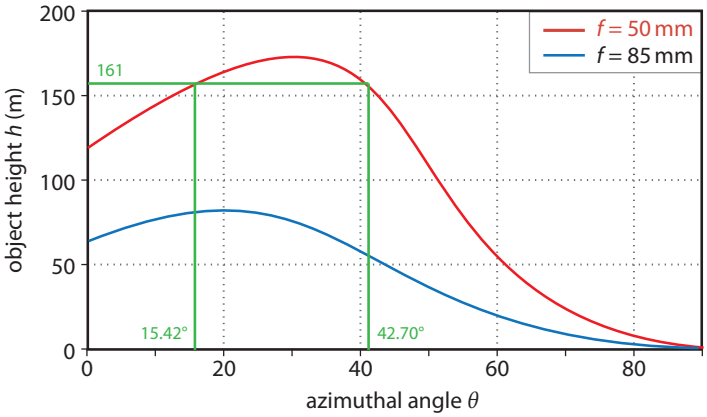

Figure S6.24b Object height h versus the angle of inclination θ for two focal lengths $f = 50$ mm and $f = 85$ mm and for a format of $h' = 6$ cm.

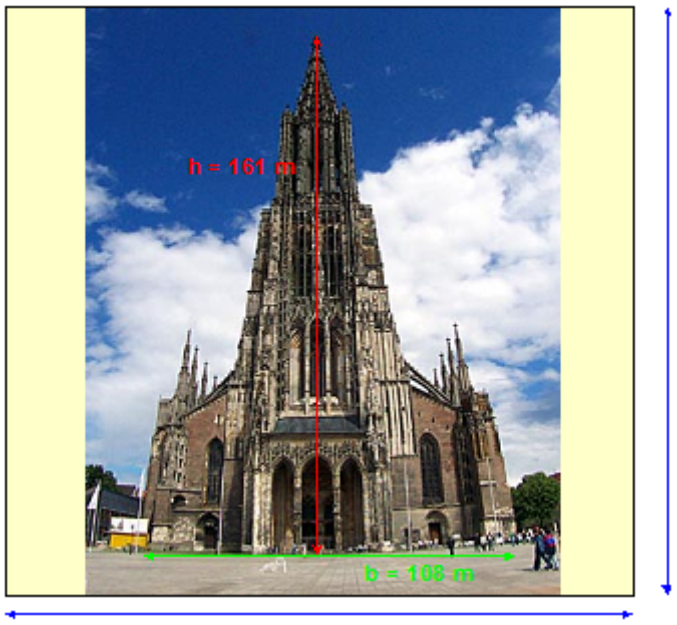

Figure S6.24c Photograph of the Ulmer Muenster taken by using a Scheimpflug camera setup.

P6.13
Direct ophthalmoscopes

In direct ophthalmoscopy, the maximum angular field of view for an emmetropic eye is given by

$$\alpha_{\mathrm{fov}} = \frac{d_{\mathrm{pupil}} + d_{\mathrm{phys}}}{L_{\mathrm{pp}}} \quad , \tag{6.83}$$

where d_{pupil} denotes the pupil diameter of the patient, d_{phys} the pupil diameter of the physician, and L_{pp} the distance between the patient's and the physician's pupil. Verify this relation by means of a drawing.

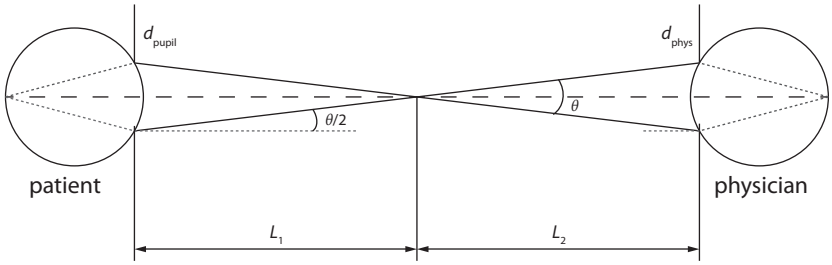

Figure S6.25 Ray diagram to illustrate the optical paths of a direct ophthalmoscope.

Solution:

We start with

$$\begin{aligned} L_1 + L_2 &= L_{\mathrm{pp}} \quad , \\ L_1 &= \frac{d_{\mathrm{pupil}}}{2\tan(\theta/2)} \quad , \\ L_2 &= \frac{d_{\mathrm{phys}}}{2\tan(\theta/2)} \quad . \end{aligned}$$

Therefore, it follows that

$$L_1 + L_2 = L_{\mathrm{pp}} = \frac{d_{\mathrm{pupil}} + d_{\mathrm{phys}}}{2\tan(\theta/2)} \quad .$$

In paraxial approximation, the angle is given by

$$\begin{aligned} \frac{\theta}{2} &= \frac{d_{\mathrm{pupil}} + d_{\mathrm{phys}}}{2L_{\mathrm{pp}}} \\ \Rightarrow \theta &= \frac{d_{\mathrm{pupil}} + d_{\mathrm{phys}}}{L_{\mathrm{pp}}} = \alpha_{\mathrm{fov}} \quad , \end{aligned}$$

which is equal to the maximum angle of the field of view.
Comment: d_{phys} can also represent the diameter of the observation aperture of the ophthalmocsope, depending on which value is smaller.

P6.14
Indirect ophthalmoscopes I

A patient with emmetropic eyes (refractive power of eye $\mathcal{D}_{\mathrm{eye}} \approx 60\,\mathrm{D}$) is examined with an indirect ophthalmoscope which uses an ophthalmoscopy lens with a refractive power of $13\,\mathrm{D}$. The free diameter of the ophthalmoscopy lens is $d_{\mathrm{oph}} = 40\,\mathrm{mm}$. The physician observes the intermediate image of the fundus from a distance of $40\,\mathrm{cm}$.

1. At which distance from the patient's eye (pupil plane) must the ophthalmoscopy lens be placed?
2. How large is the field of view d_{fov} on the retina?
3. How large would the field of view be for a direct ophthalmoscope (same distance between patient and physician; pupil diameter of patient is $7\,\mathrm{mm}$; pupil diameter of physician is $3\,\mathrm{mm}$)?

Solution:

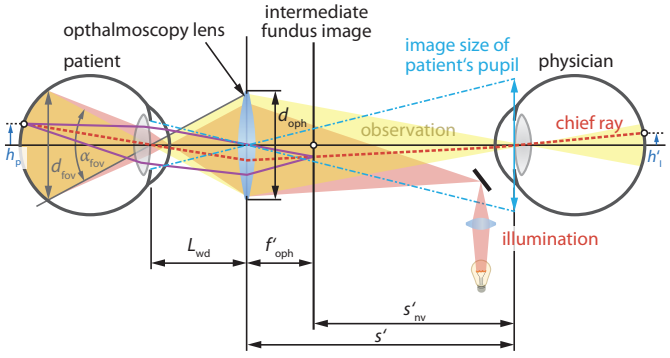

Figure S6.26 Ray diagram of an indirect opthalmoscope which shows the illumination beam path (red) and the observation path (yellow).

1. As the near-viewing distance $s'_{\rm nv}$ we use the distance of the intermediate image to the observer (40 cm). Thus, we have

$$\begin{aligned}\mathcal{D}_{\rm oph} &= \frac{1}{f'_{\rm oph}} = 13\ {\rm D}\ ,\\ f'_{\rm oph} &= \frac{1}{\mathcal{D}_{\rm oph}} = 7.7\ {\rm cm}\ ,\\ \mathcal{D}_{\rm eye} &= \frac{1}{f_{\rm eye}} = 60\ {\rm D}\ .\end{aligned}$$

In a 4-f system, the distance of ophthalmoscopy lens from the physician's eye is therefore

$$s' = f'_{\rm oph} + s'_{\rm nv} = 47.7\ {\rm cm}\ .$$

In order to have the patient's pupil imaged into the physician's pupil, we calculate with lens equation (A14)

$$\begin{aligned}\frac{1}{s'} - \frac{1}{L_{\rm wd}} &= \mathcal{D}_{\rm oph}\ ,\\ \Rightarrow L_{\rm wd} &\approx -9.2\ {\rm cm}\ .\end{aligned}$$

The opthalmoscopy lens must thus be placed 9.2 cm away from the patient's pupil plane.

2. With the parameters

$$\begin{aligned}d_{\rm oph} &= 4\ {\rm cm}\ ,\\ L_{\rm wd} &= -9.2\ {\rm cm}\ ,\end{aligned}$$

we have – according to Eq. (6.72) – the field of view given by $d_{\rm fov} \approx \alpha_{\rm fov}/\mathcal{D}_{\rm eye}$ and on the other hand, from Figure S6.26, the relation

$$\alpha_{\rm fov} \approx \frac{d_{\rm oph}}{L_{\rm wd}} = 0.435\ {\rm rad}\ .$$

Thus, it follows that

$$d_{\rm fov} \approx \frac{\alpha_{\rm fov}}{\mathcal{D}_{\rm eye}} = \frac{0.435}{60\ {\rm D}} \approx 7.25\ {\rm mm}\ .$$

3. We compare this with a direct ophthalmoscope (see Problem P6.13) and obtain

$$\begin{aligned}L_{\rm pp} &= L_{\rm wd} + s' = 56.9\ {\rm mm} \approx 57\ {\rm mm},\\ \alpha_{\rm fov} &= \frac{d_{\rm pupil} + d_{\rm phys}}{L_{\rm pp}} = \frac{7\ {\rm mm} + 3\ {\rm mm}}{57\ {\rm mm}} \approx 0.175\\ \Rightarrow d_{\rm fov} &\approx \frac{\alpha_{\rm fov}}{\mathcal{D}_{\rm eye}} \approx 0.3\ {\rm mm}\ .\end{aligned}$$

Hence, in a direct ophthalmoscope, the field of view is about $24\times$ smaller.

P6.15
Indirect ophthalmoscopes II

An eye is examined with an indirect ophthalmoscope. The distance between patient and physician is $50\,\text{cm}$ and the ophthalmoscopy lens is placed at a distance of $5\,\text{cm}$ in front of the patient's eye.
1. Determine the required refractive power of the ophthalmoscopy lens.
2. Calculate the diameter of the image of the patient's pupil (originally $4\,\text{mm}$) in the plane of the physician's pupil.
3. At which magnification does the physician observe the fundus (refractive power of patient's eye $\mathcal{D}_{\text{eye}} \approx 60\,\text{D}$)?

Solution:

1. We have

$$\begin{aligned} L_{\text{wd}} &= 5\ \text{cm}\ , \\ L_{\text{pp}} &= 50\ \text{cm}\ , \\ s' &= L_{\text{pp}} - L_{\text{wd}} = 45\ \text{cm}\ . \end{aligned}$$

   Using the lens equation leads to

$$\begin{aligned} \frac{1}{f} &= \frac{1}{s'} + \frac{1}{s} \\ \Rightarrow \frac{1}{f} &= \frac{1}{s'} + \frac{1}{L_{\text{wd}}} = \frac{2}{9}\ . \end{aligned}$$

   Therefore, it follows that $f = 4.5\,\text{cm}$. The power of the ophthalmoscopy lens is thus

$$\mathcal{D}_{\text{oph}} = \frac{1}{f} = \frac{2}{9\ \text{cm}} = \frac{2}{9 \times 10^{-2}\,\text{m}} = 22.2\ \text{D}\ .$$

2. From Figure S6.26, we find the relation

$$\begin{aligned} \frac{s'}{L_{\text{wd}}} &= \frac{d_{\text{image}}}{d_{\text{pupil}}} \\ \Rightarrow d_{\text{image}} &= 36\ \text{mm}\ . \end{aligned}$$

   The diameter of the image of the patient's pupil (which is originally $4\,\text{mm}$) in the plane of the physicians's pupil appears to be $36\,\text{mm}$.

3. The magnification of an indirect ophthalmoscope is given by Eq. (6.73) and has a value of

$$\beta = -\frac{\mathcal{D}_{\text{eye}}}{\mathcal{D}_{\text{oph}}} = -\frac{60\ \text{D}}{22.2\ \text{D}} = -2.702 \times \quad .$$

   Thus, the fundus can be viewed with a magnification of about $3\times$.

P6.16
Indirect ophthalmoscopes III

The fundus of a patient shall be examined with an indirect ophthalmoscope. The pupil diameter of the patient has been enlarged to 7 mm. The ophthalmoscopy lens has a refractive power of 30 D and is placed at a distance of 50 cm in front of the physician's eye. The physician has an interpupillary distance of $\mathrm{PD} = 65\,\mathrm{mm}$. Is it possible for the physician to perceive a virtual stereoscopic image of the patient's fundus or does he require an optical device which effectively reduces PD?

Solution:

We start with

$$\begin{aligned} s' &= 50\ \mathrm{cm}\ , \\ d_{\mathrm{pupil}} &= 7\ \mathrm{mm}\ , \\ \mathcal{D}_{\mathrm{oph}} &= \frac{1}{f} = 30\ \mathrm{D}\ , \\ \mathrm{PD} &= 65\ \mathrm{mm}\ . \end{aligned}$$

Inserting these values into the the paraxial lens equation (A14) leads to

$$\begin{aligned} \frac{1}{s'} - \frac{1}{L_{\mathrm{wd}}} &= \mathcal{D}_{\mathrm{oph}}\ , \\ \frac{1}{L_{\mathrm{wd}}} &= \frac{1}{s'} - \mathcal{D}_{\mathrm{oph}} = -28\ \mathrm{m}^{-1}\ , \\ L_{\mathrm{wd}} &= \frac{-1}{28\ \mathrm{m}} = -3.6\ \mathrm{cm}\ . \end{aligned}$$

The transverse magnification is calculated, according to Eq. (A15), to

$$\beta = \frac{s}{s'} = \frac{s'}{-L_{\mathrm{wd}}} = -\frac{50\ \mathrm{cm}}{3.6\ \mathrm{cm}} = -13.9\times\ \approx\ 14\times\ .$$

Thus, the diameter of the image of the patient's pupil in the observer's pupil results as

$$d'_{\mathrm{pupil}} = \beta d_{\mathrm{pupil}}\ \approx\ 14 \cdot 7\ \mathrm{mm} = 98\ \mathrm{mm}\ .$$

The diameter of the image of the patient's pupil in the observer plane is thus larger than his pupillary distance PD. This allows the physician viewing the patient's retina simultaneously with both eyes (binocular vision). He thus has a stereoscopic impression of the patient's fundus. An additional optical device to reduce the PD is not required. In effect, the physician actually "does" a so-called "pupil splitting" by selecting a pupil range out of the aerial image plane.